CHALMERS
UNIVERSITY OF TECHNOLOGY

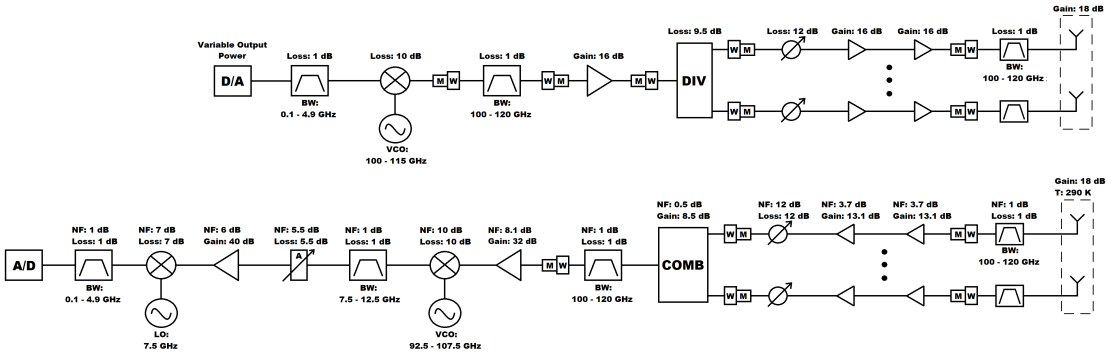

Communication systems beyond 100 GHz

Link- and system-budget analysis of a communication system and FMCW radar operating beyond 100 GHz

Master's thesis in Communication Engineering & Wireless, Photonics and Space Engineering

JAKOB GUSTAVSSON
GUSTAV HENRIKSSON

DEPARTMENT OF ELECTRICAL ENGINEERING

CHALMERS UNIVERSITY OF TECHNOLOGY
Gothenburg, Sweden 2022
www.chalmers.se

Master's thesis 2022

Communication Systems beyond 100 GHz

Link- and system-budget analysis of a communication system and FMCW radar operating beyond 100 GHz

Jakob Gustavsson and Gustav Henriksson

CHALMERS
UNIVERSITY OF TECHNOLOGY

Department of Electrical Engineering
Division of Communication Systems
Chalmers University of Technology
Gothenburg, Sweden 2022

Communication systems beyond 100 GHz

Link- and system-budget analysis of a communication system and FMCW radar operating beyond 100 GHz
Jakob Gustavsson, Gustav Henriksson

Supervisors:
Johan Wettergren, Qamcom
Jafar Banar, Department of Electrical Engineering

Examiner:
Thomas Eriksson, Department of Electrical Engineering

Master's Thesis 2022
Department of Electrical Engineering
Division of Communication Systems
Chalmers University of Technology
SE-412 96 Gothenburg

Cover: Schematic for a Communication system beyond 100 GHz, with separate transmitter and receiver architectures.

Typeset in LaTeX
Printed by Chalmers Reproservice
Gothenburg, Sweden 2022

Abstract

As the demand for information exchange grows, the currently used frequency bands become increasingly crowded and higher communication rates are desired. In an effort to combat this, there is a drive to utilize higher frequencies with larger bandwidths than what are currently used. Doing so is however not easy, as there is a lack of commercially available hardware available for such frequencies while pathloss and shadowing affect high frequencies more drastically. This work has aimed to conduct a realistic link- and system-budget analysis of a theoretical communication system with 2 variations to the antenna setup, as well for a theoretical frequency modulated continuous wave radar system, both functioning above 100 GHz. The baseline case for the communication system consists of two separate chains for transmitting and receiving, while the variations consider a smaller antenna with less directional gain and a system utilizing a shared antenna. In order to construct these theoretical systems, components developed by the international collaboration ENTRY100GHZ have been used when available. For components not developed by the ENTRY100GHZ collaboration, reasonable values based on currently existing or experimental hardware has been used. When considering the propagation of the signal, the close-in model has been used. The parameters considered for performance evaluation are third order intermodulation products, noise spectral density and signal power. These parameters are then used in order to estimate at what ranges certain modulations, and therefore what theoretical throughputs, are available on said channel model. The initial communication system achieves theoretical maximum rates of between 3.3-16.8 Gbits/s, where the lowest obtainable rate is available for ranges between 0.5 and 47.3 m while the highest rate is available for ranges 1.2-9.8 m. For the communication system variations, the lowest rate is available at ranges of 0.2-22.4 m and 0.6-30.5 m, while the highest rate is available between 0.6-4.6 m and 1.4-6.2 m for the smaller and switched antenna cases respectively. For the frequency modulated continuous wave radar case, a sufficient detection range between 1.0 and 161.1 m is achieved with a range resolution of ± 0.3 m, a velocity resolution of ± 1.0 m/s and a maximum unambiguous velocity of 55.4 m/s. These results show that communication and frequency modulated continuous wave radar systems are indeed possible on frequencies beyond 100 GHz. For the communication system, high wireless rates are obtained while the radar enjoys decently high resolutions and detection ranges for the intended application.

Keywords: sub-THz, W-band, FMCW radar, Communication system, system-budget, link-budget.

Acknowledgements

Throughout the work with this project, many people have aided in making it the best it could be. Firstly we would like to thank our advisor Johan Wettergren at Qamcom for commissioning the thesis and providing guidance with all parts of the work. Secondly, we would like to thank our examiner Thomas Eriksson at Chalmers for providing feedback on the report as well as the thesis presentation. We would like to thank our advisor at Chalmers Jafar Banar for aiding us with our report. Lastly, we would like to thank all members of the ENTRY100GHZ collaboration for sharing their work with us, enabling us to perform ours.

Jakob Gustavsson and Gustav Henriksson, Gothenburg, June 2022

List of Acronyms

EHF	Extremely High Frequency
FMCW	Frequency-Modulated Continuous-Wave
OIP3	Output Third Order Intercept Point
IEEE	Institute of Electrical and Electronics Engineers
CI	Close-in
FEC	Forward Error Correction
LDPC	Low Density Parity Check
RS	Reed-Solomon
RC	Raised Cosine
PSK	Phase-Shift Keying
BPSK	Binary Phase-Shift Keying
QPSK	Quadrature Phase-Shift Keying
APSK	Amplitude Phase-Shift Keying
QAM	Quadrature Amplitude Modulation
IF	Intermediate Frequency
RF	Radio Frequency
AM	Amplitude Modulation
FM	Frequency Modulation
PAPR	Peak to Average Power Ratio
SNR	Signal to Noise Ratio
BER	Bit Error Rate
EVM	Error Vector Magnitude
DAC	Digital to Analog Converter
ADC	Analog to Digital Converter
PSD	Power Spectral Density
NF	Noise Figure
LO	Local Oscillator
VCO	Voltage Controlled Oscillator
PLL	Phase-Locked Loop
LNA	Low Noise Amplifier
LOS	Line Of Sight
PLE	Path Loss Exponent
SF	Shadow Fading
Tx	Transmitter
Rx	Receiver
FDD	Frequency Division Duplexing
TDD	Time Division Duplexing

Contents

List of Figures

List of Tables

1
Introduction

Crowded frequency bands [1],[2] in combination with an increasing demand for high data rates mean there is a desire to expand practically realizable frequencies beyond what is currently possible. Realizing large scale EHF communication is a key enabler for many applications, including information showering, intra-device links, wireless front- and back-haul and wireless data centers among others[3],[4]. There already exist communication systems on EHF frequencies [5],[6], although they are not yet wide-spread. This gives reason to further investigate and explore them as practically realizable on a larger scale, possibly in a more portable format. In order to achieve this, however, there is a need of development for compatible hardware and signal processing [7].

This thesis is part of the international collaboration ENTRY100GHz[8], which stretches several years. Within the collaboration, several partners from Europe and Africa are responsible for specific hardware components for a communication system operating on frequencies between 100-120 GHz. The hope is to then utilize these components in order to construct a functioning communication system on said frequencies. To gain a realistic view of the system performance, this work aims to conduct a link and system analysis of the system in development, providing the ENTRY100GHz collaboration with valuable information about the overall link quality. Additionally, a comparison between a communication system and FMCW radar should be made. This is because these types of systems have a similar structure, while FMCW radar also benefits from the large bandwidths possible at EHF.

By providing this overall view of the system, it is possible to quantify how it is expected to perform in terms of signal quality. This will in turn simplify discussions between the partners regarding performance of every single component in the system, along with how they interact with each other. Additionally, studying variations of the system allows their drawbacks and advantages to be identified. Lastly, this overview will allow realistic estimations regarding link quality and throughput.

2
Theory

2.1 Digital Processing Block

The digital processing block is the first and last block of a communication system, illustrated in figure 3.1. On the transmitter side, this block is responsible for constructing the initial digital base band signal. On the receiver side, it is responsible for handling the digital processing of the received signal.

2.1.1 Channel coding

While transmitting information over a channel there is, in practice, always a risk of losing information along the way due to various channel disturbances. This is especially true for wireless channels, as it is not an easily controllable environment. In order to reduce the errors which occur during transmission it is possible to apply a few different measures. One such measure is to make use of channel coding. In this section, a brief description of the main idea behind some coding is given.
The main idea of channel coding is to add some redundant information to the original message. The most basic type of coding would be to add a parity bit to the message, where the parity bit ensures an even or odd amount of 1's or 0's for any given message. Using such a code, it is only possible detect an odd amount of errors within the message, although it is never able to correct any of them. However, there exist codes with the capability to correct some errors, known as FEC code. If the code has FEC-capabilities, some errors can be handled at the cost of some throughput. Because of this, one can use the notion of coding gain, which is a description of how much transmit power the error correction capabilities correspond to[9]. In other words, it is a description of how much less energy can be used in transmission while still achieving similar error-rates with the FEC-code. Although coding can improve the performance of a communication system, they also add complexity. An advanced, high performance decoder requires valuable space on a given chip, while design and cost keep the operating frequency upper bounded to about 1 GHz[10]. If higher rates are to be achieved, the expended energy per decoded bit needs to decrease inversely proportionally to the increased throughput[10].

2.1.2 Pulse Shaping

In order to achieve communication over a wireless channel, there needs to exist some analog wave carrying information over the channel itself. The first idea which comes to mind is to utilize a square-pulse, although its large bandwidth[11] cause it to be a

poor choice of pulse to carry the information. Instead, there exist a need for pulses which require as small bandwidth as possible, while not causing enough interference to neighboring transmissions to make them unintelligible. One such type of pulse is the Nyquist-pulse[12], which can be described mathematically by

$$v(nT) = 0, n = \pm 1, \pm 2..., v(0) \neq 0 \tag{2.1}$$

The optimal-bandwidth pulse which fulfills the criteria given in equation 2.1 is the sinc(t)-pulse[11]. This pulse, however, is not practically usable due to its non-causality in combination with its frequency-domain discontinuities, meaning it is difficult to realize in practice. Because of this, other pulses which are causal and lack frequency-domain discontinuities are used, such as the RC and BTN pulses[13]. These pulses, while having a less desirable frequency spectrum, are more easily realized in practice while having a similarly narrow spectrum when compared to the sinc(t)-pulse.

2.1.3 Carrier Synchronization

There are several influencing factors that degrade the signal along its path between the baseband in the transmitter and the baseband in the receiver. Among these factors are phase noise, carrier frequency and carrier phase offsets. The phase noise originate from the oscillators used in the system and their frequency precision. The carrier phase offset is due to the analog wave propagation through the transmitter blocks, the channel and the receiver blocks. The carrier frequency offset is mainly due to conversion errors that occur in the down-conversion of the carrier wave[14]. These effects will impact the phase of the originally transmitted symbols such that they end up having a different phase in the receiver. The phase noise will apply a random phase offset to each received symbol. The frequency offset will induce a time varying phase offset since phase is the integration of frequency with respect to time. Because of this, the combination of these offsets will result in a phase offset that contains both a constant and a time varying term[15]. The observed phase offset of the received symbols in the receiver baseband is presented in equation 2.2.

$$\theta(t) = 2\pi\Delta f t + \theta_0 + N_{phase} \tag{2.2}$$

where Δf is the frequency offset after the down-conversion, θ is the constant phase offset and N_{phase} is the phase noise.

In coherent communication systems, phase information is used in order to map the received symbols to the correct constellation point. Therefore, the ability to compensate for carrier frequency and phase offsets are crucial for the receiver in such systems. A large enough phase offset will cause the received symbol to appear outside of the intended constellation point's decision region, resulting in an incorrect mapping of the symbol. Figure 2.1 illustrates an example of this effect for a 16-QAM constellation.

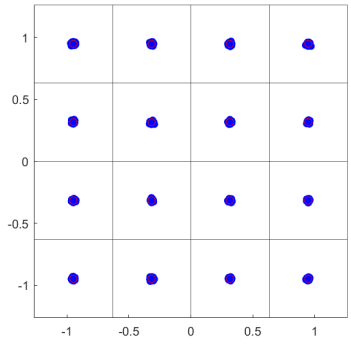

(a) 16-QAM constellation.

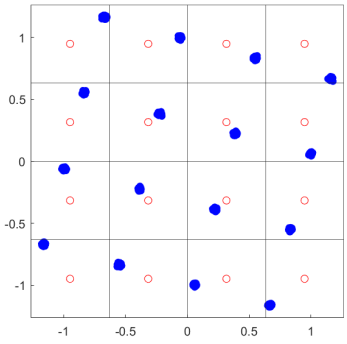

(b) 16-QAM constellation with phase error.

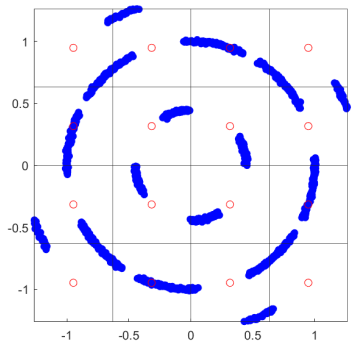

(c) 16-QAM constellation with phase and frequency error.

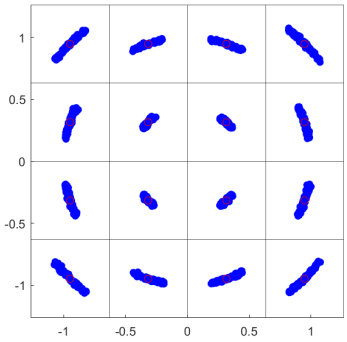

(d) 16-QAM constellation with phase noise.

Figure 2.1: Illustration of phase and frequency error effects on a 16-QAM constellation. The constellations are simulated with additive white Gaussian noise to have an SNR of 40 dB.

The digital processing block can utilize different methods in order to compensate for carrier frequency and phase offsets. Since the phase noise originates in the oscillators, this effect is difficult to compensate for with digital processing and will be further mentioned in relation to the oscillators. Carrier frequency offsets can for example be estimated using digital frequency-locked loops which detect phase differences as a function of time in order to determine the frequency offset[15]. Carrier phase offsets can also be estimated by comparing the expected pilot symbols with the received pilot symbols. This comparison of pilot symbols can only be made when the pilot symbols are known to the receiver, which is often the case[16].

2.1.4 Timing Synchronization

Timing is a crucial part of communication. At the base band frequency, the signal will at the time of transmission contain symbols which are separated by the symbol time interval. After transmission and reception, the signal will be observed at the receiver base band with a time delay due to propagation. This time delay can be

described as a multiple of the symbol time interval plus an additional delay that is smaller than the symbol time delay. This additional delay is referred to as the timing phase[15]. The time when the signal reaches the receiver base band can be written as equation 2.3.

$$t_{rx} = t_{tx} + mT + \tau \tag{2.3}$$

In equation 2.3, t_{tx} is the time when the signal is transmitted, m is a positive integer, T is the symbol time interval and τ is the timing phase. An incorrect timing phase will negatively affect the receiver's ability to utilize samples at the optimum points in time, leading to an overall decrease in system performance.
Estimation of timing phase can be performed with maximum likelihood based functions in the receiver[15]. These functions compare the samples obtained in frames of the symbol time interval and determines the sample with the highest possible average symbol energy. The offset in samples from these functions serve as an estimate of the timing phase. This enables the receiver to choose the optimum sample points for de-mapping the symbols, effectively compensating for the timing phase.

2.1.5 Modulation

The format for transmitted information is, most commonly, binary. Because of this, there is a need to in some way transform binary bit-sequences into an analog signal which can be transmitted on a channel using some analog pulse. However, simply having a single analog pulse yields no information in itself, but there is instead a need to modify the pulse in a way that makes it carry some information. To achieve this, the bits are modulated onto a finite set of constellation points, where the number of bits assigned to each point depends on the modulation-order of the chosen modulation scheme. Assuming that every symbol in a constellation can carry an equal number of bits, the number of bits each symbol can carry is modeled by[11]

$$n = log_2(M) \tag{2.4}$$

where M is the number of symbol constellation points in the given modulation scheme.
The way that a given symbol actually modifies the analog pulse used to carry information varies with modulation schemes and there are three basic categories. Firstly, there are amplitude-modulation schemes where, as the name implies, the amplitude of the signal is modified to carry some information. Secondly, frequency modulation modifies the frequency of the signal in order to make it distinguishable and hence carry information. Lastly, there is the possibility to modify the phase of the signal in order to make it carry information. These three basic types of modulation can then be combined to form various modulation schemes which combine these concepts, such as M-QAM which utilizes both amplitude and phase to modulate information onto a carrier[11]. Constellations such as BPSK, QPSK and 8-PSK are constant-envelope constellations, meaning all the constellation points have the same distance from the origin[11] or, equivalently, that no information is contained within the amplitude.For non-constant envelope constellations, if the same peak transmission power is imposed, the average power of the constellation points will in fact be lower,

affecting link-quality negatively. This discrepancy between the peak transmission energy and average transmission energy is specified by PAPR[17].

The 8-APSK and 16-QAM constellations are as previously mentioned not constant-envelope constellations, meaning they have PAPR<1. Since the BER-curves in figure 2.2 has $\frac{E_s}{N_0}$ in average transmission power, the 8-APSK and 16-QAM constellations will need to take PAPR into account to be comparable to the constant-envelope constellations. The PAPR can be calculated using equation 2.5 from [17].

$$PAPR[dB] = P_{peak} - P_{average} \tag{2.5}$$

where P_{peak} and $P_{average}$ are the maximum and average transmission powers in dBm respectively. For the constant envelope constellations, the average transmission power is equal to the peak transmission power, as the same power is associated with every modulation point. For the non-constant-envelope modulations, assuming the constellation points are equally likely, the average transmission power is calculated using equation 2.6 obtained from [11].

$$P_{average}[W] = \sum_{i=1}^{M} P_{point} \cdot P_{likelihood} = \sum_{i=1}^{M} d_i^2 \cdot P_{likelihood} = \frac{1}{M} \sum_{i=1}^{M} d_i^2 \tag{2.6}$$

Where M is the number of points in the constellation, $P_{likelihood}$ is the probability of transmitting a specific constellation point and d_i is its distance from the origin. For the case of equally likely symbols in 16-QAM, the PAPR turns out to be 2.55 dB, while the 8-APSK case yields a PAPR of 2.13 dB. This means that the average transmission energy for those constellations will be 2.55 dbm and 2.13 dBm lower, meaning more favorable conditions need to hold in order to efficiently use them. In order to ensure that the required SNR for a given constellation is comparable between all of the constellations, the peak SNR will be used instead of the average SNR. This way, the deterioration in availability due to the PAPR is easily visualized.

In order to achieve communication with a certain quality, a reasonable bit error-rate needs to be determined. The bit error-rate is dependent on SNR and modulation. For a few commonly used modulations, a BER-curve is shown in 2.2.

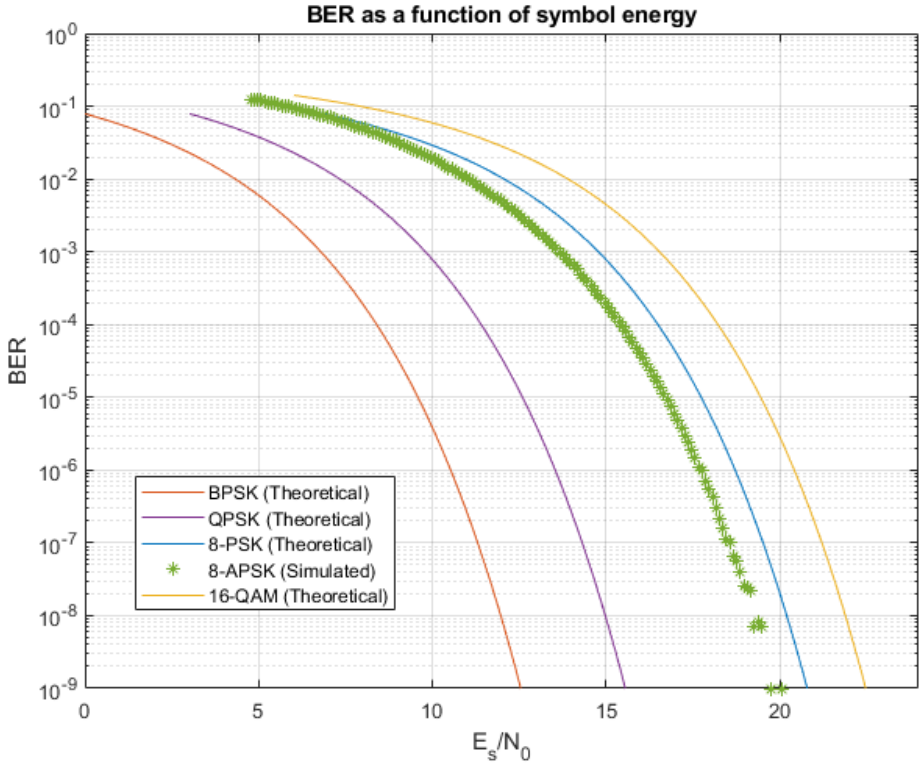

Figure 2.2: BER as a function of average SNR for each symbol, $\frac{E_s}{N_0}$

2.1.6 Throughput

Throughput is a commonly used parameter for describing system-performance. In order to describe the theoretically maximal throughput, some things need to be considered. Firstly, the symbol rate (baud rate) can be described by 2.7[11]

$$R_s = B \tag{2.7}$$

where B is the bandwidth of the system, excluding the guard-band. Secondly, the modulation order of each individual symbol must be considered, as the number of constellation points is proportional to the number of bits carried on a symbol as in equation 2.4. Lastly, the coding used in the transmission of the symbols are of importance, as it yields some overhead regardless of what type of frame is being sent. These effects result in a maximum throughput using equation 2.8

$$Throughput = R_s \cdot log_2(M) \cdot C/R \tag{2.8}$$

where C/R is the code-rate. This throughput does not take into consideration any overhead which is not due to coding, such as pilot-frames. Neither does it consider error rates related to link SNR. It also assumes that the communication is simplex or synchronous, meaning there is no back-off time needed and the channel can be used 100% of the time. Because of these assumptions, the system should never be expected to transmit at the stated rates, they should instead be seen as an upper bound of what is possible under ideal conditions.

2.2 Mixed signal Block

In order to successfully utilize a digital communication system, there needs to be some way to convert digital signals into analog ones and vice versa. These processes are done using a DAC and an ADC respectively.
A simple version of an ADC can be seen in figure 2.3 which consists of a filter, sampler, clock and quantizer. The main idea behind an ADC is that some analog signal exists at the input of a sampler, which samples the signal with some frequency f_s provided by a clock. The sampled, analog values are then discretized by a quantizer, mapping the analog value onto a discrete set of quantizable values. The quantized values are then utilized in digital processing. In the case of a DAC, the process is similar but inverted.

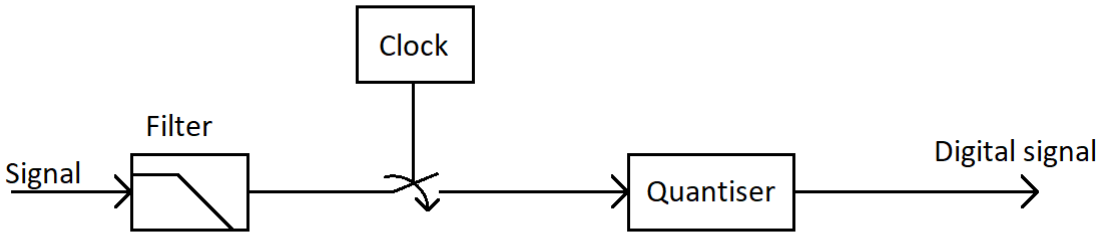

Figure 2.3: Simplest form of an ADC, where an analog signal is passed through a filter, sampled and then finally quantized.

2.2.1 Sampler

The main purpose of a sampler is to pick out a finite set of values from an otherwise possibly infinite sequence of values, discretizing it with respect to time. In general, higher sampling frequencies are advantageous as it allows for wider bandwidths to be represented, while smaller bandwidths can still be attained by utilizing filtering. Further, if less data is desirable compared to the sample rate downsampling can be employed to reduce the amount of samples, making lower sampling rates artificially attainable without modifying the clock frequency.
A known problem in any given signal-acquisition system is the issue of undesirable signals folding into the band of interest, known as aliasing. This is usually largely removed using an analog anti-aliasing filter before the sampler as indicated in figure 2.3. However, having an ideal analog filter is not realizable and high performance filters are often costly. Due to this, there will always be some undesired signals left in the filtered signal.

2.2.2 Clock

The first important parameter for the clock is sample jitter. The jitter is a measurement of how much the timing deviates on a sample-to-sample basis. In other

words, if sample a_i is supposed to be taken at time t_i, it will instead be taken at time $t_i + \Delta t_i$ where Δt_i is the jitter associated with sample i. This timing jitter will result in the signal being sampled at a different time than intended, effectively adding some noise to the sample as can be seen in figure 2.4. This effect is more severe at higher frequencies, as the signal amplitude then varies more swiftly, meaning the amplitude will change more during the jitter time. In the case of a pure sine wave $Asin(\omega t)$ for example, without any noise present, the jitter-noise can be modeled by

$$\Delta X(nT) = A\omega cos(\omega t)\delta(nT) \tag{2.9}$$

assuming the derivative of the signal does not significantly change over the jitter time or, equivalently, that the jitter time is sufficiently small in comparison to the second derivative of the signal. The frequency-dependency seen in equation 2.9 means that clock-jitter will be a major concern in the design of sub-THz systems, as even a small jitter can potentially ruin the signal reception entirely. Further, the amplitude dependency means that even if a higher transmit power is used it will not increase the signal quality with respect to the jitter.

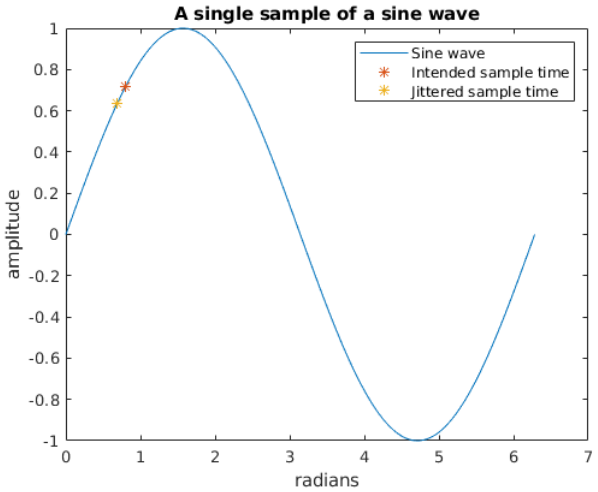

Figure 2.4: figure depicting the phenomena of jitter, where the actual sample point deviates from the intended one.

In order to perform the sampling swiftly enough, the clock frequency controlling the sampling speed is obviously of importance. The lowest such frequency required to accurately reconstruct the sampled signal, known as the Nyquist frequency, can be calculated using equation 2.10, where f_{band} is the bandwidth of the signal

$$f_s = 2f_{band} \tag{2.10}$$

This is, however, a lowest-requirement in an ideal world where perfect filters exist and no other disturbances affect signal reception/down-conversion, meaning that f_s in reality needs to be higher. How much higher depends on the type of filter used, along with its filter order, harmonic distortion requirements and so on. However, if cost and size can be ignored, higher sample rates are generally desired.

2.2.3 Quantizer

Once the analog signal has been sampled, there is a need to discretize the samples with respect to amplitude. This is done using a quantizer, where the analog amplitude is typically mapped to the closest of a finite set of quantizable values. The number of quantizable levels is often expressed in terms of bits using

$$n = 2^N \tag{2.11}$$

where n is the number of quantizable levels and N is the number of bits associated with the quantizer.
Since the quantizer maps an analog signal onto an alphabet with a finite number of values, there will undoubtedly be some discrepancy between the quantized and true value, as can be seen in figure 2.5. This discrepancy can, in the case of a full-range sine signal, be modeled as additive noise, provided the quantization steps are of equal length while a sufficiently large number of bits are used to quantize and the input is not correlated to the error[18]. If only this quantizer-noise is considered for a full-range sine wave, the SNR of an N-bit quantizer can be modeled as in equation 2.12[18],[19]. It is, however, important to realize that the quantizer itself does not add to the signal quality. Instead, the SNR measurement should be seen as how well the quantizer can represent the given signal. In other words, the goal is to have a quantizer which is good enough to not limit the signal quality noticeably, while at the same time keeping it simple enough to be cost-effective.

$$SNR = 6.02N + 1.75dB \tag{2.12}$$

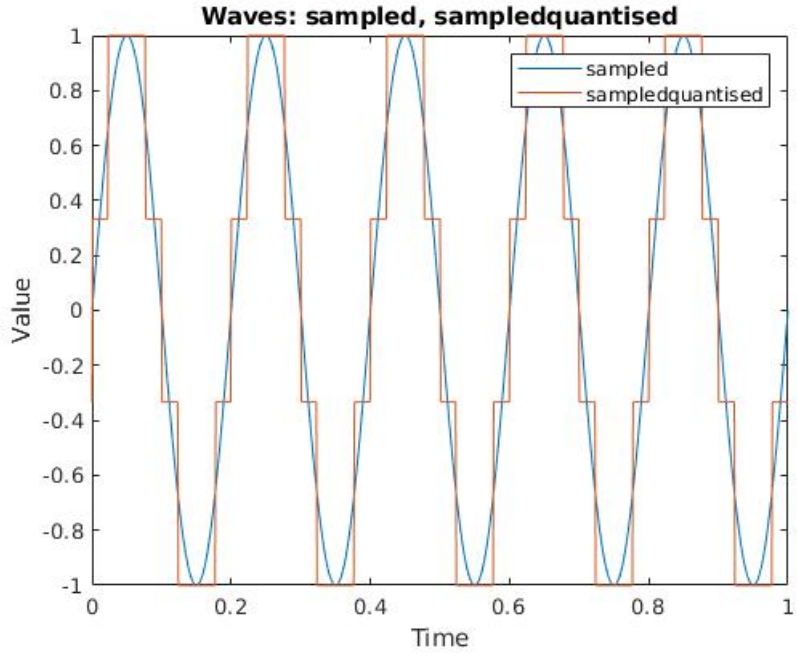

Figure 2.5: Image showing a sampled and sampled + quantized version of a 5 Hz sine wave, using sampling frequency $f_s >> f_{Nyquist}$. Here, the discrepancy between the 2-bit quantized and the sampled signal is clearly visible.

In order to model the quantization noise which the ADC incurs on the signal as in [18], some properties regarding the signal and quantizer will be assumed to hold true. The first is that all of the quantization levels are utilized with equal probability, which is assumed to hold true for this case. Secondly, a sufficiently large number of quantization levels needs to be present. Although how large is never specified, it is stated that it holds for "most cases", meaning 12-bit ADC's, which are commonly used, are assumed to fulfill this requirement. Third, the quantization steps should be uniform. According to the specifications of the chosen ADC[20], this should also be the case and it will be assumed that the specified INL and DNL hold true for this case. Lastly, the quantization error needs to be uncorrelated with the input, which is also assumed to hold true. If all these things hold true, the quantization noise power can be calculated using

$$P_Q = \frac{\Delta^2}{12} \tag{2.13}$$

where

$$\Delta = \frac{V_{pp}}{2^n - 1} \tag{2.14}$$

where n is the number of bits used in the quantizer and V_{pp} is the peak-to-peak voltage range of the ADC. This noise can be considered white [18], meaning its power spectrum spreads throughout the whole Nyquist band. Following this, the PSD of the noise can be expressed as equation 2.15.

$$PSD_Q = \frac{\Delta^2}{6f_s} \tag{2.15}$$

If the signal to be quantized is not full-range, there are 2 different scenarios. The first is that the signal has lower-than-full-range amplitude, meaning the signal will never reach the full range but rather stay below it. In this case, the interval in which it is located can be considered as the full range, although not all the bits in the quantizer will be used. Instead, only a subset of all the bits will be used, where the used bits can be modeled by

$$N = log_2(n) \tag{2.16}$$

where n is the total number of quantizable levels spanned by the signal. In other words, if the signal has a smaller amplitude than the full-range, it will lead to a decrease in SNR at the quantizer, possibly ruining the system. If the signal instead overshoots the full range of the quantizer, something known as clipping occurs. What this means is that if the signal overshoots the maximum level, further increasing the signal amplitude (increasing the transmission power) will result in a worsened SNR. This is because while the signal is being overshot, the maximum-amplitude quantization point will be used, even though the actual amplitude is much higher than that level. In essence, this can be thought of as a significant quantization noise being added to the signal. A figure illustrating the impact which this phenomena has on the SNR can be seen in 2.6.

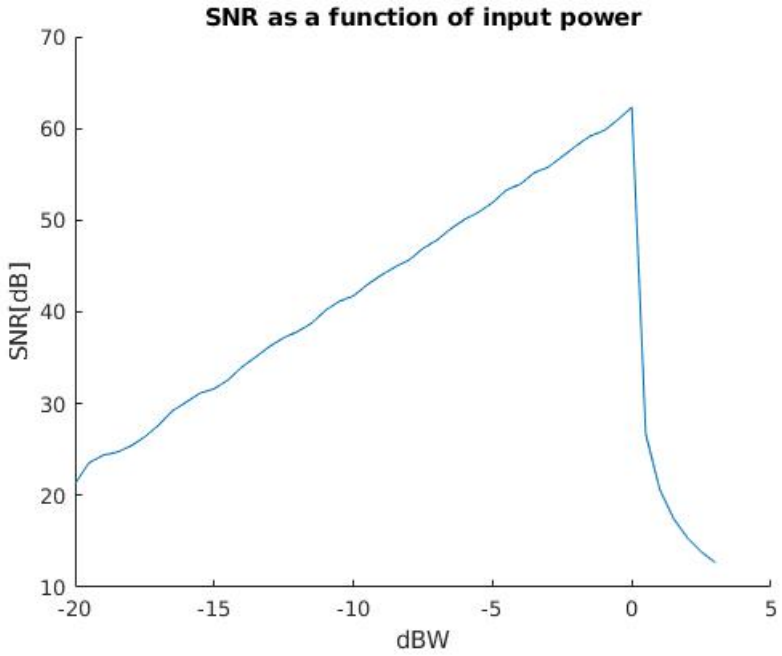

Figure 2.6: Example of SNR at quantizer using 10 bits, with sweeping input power. Here, 0 dBw = full range. At full-range, the SNR is approximately 62 dB.

2.3 IF - RF Conversion Block

Frequency conversion needs to be performed in order to move the IF signal to the RF band before it is transmitted on the desired frequency band. Similarly, frequency conversion is also necessary for bringing the received RF signal down to the IF band before sampling can be performed. Both of these processes are handled by the IF-RF conversion block. This block consists of two parts where one part handles the up-conversion in the transmitter and the other part handles the down-conversion at the receiver. Examples of both parts that make up the IF-RF conversion block can be viewed in figure 2.7.

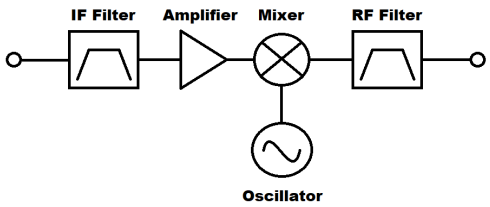

(a) IF - RF conversion block in the transmitter.

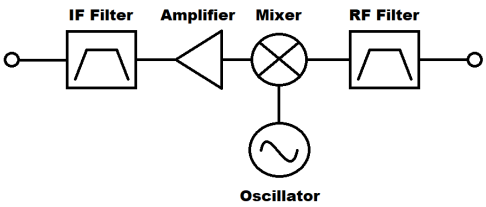

(b) RF - IF conversion block in the receiver.

Figure 2.7: Illustration of transmitter and receiver frequency conversion blocks.

Figure 2.7 illustrates that these two parts are made up of different microwave components. Here, the bandpass filters are presented as rectangles with a rectangular

pulse inside, the amplifiers are denoted as triangles turned on their sides, the mixers are represented as circles with crosses and the oscillators are illustrated as circles with sine waves inside of them. It is worth noting that these parts may differ in the amount and placement of certain components. The possible difference in components is due to the fact that there are different considerations that need to be taken into account in the transmitter and in the receiver[21]. However, these parts are similar in that they both utilize a mixer and oscillator combination to perform the frequency conversions.

This section will provide general information about the mixer and oscillator components. Filters and amplifiers will not be covered in this section since these components are covered in later chapters. This section will also explore the different considerations that need to be taken into account when designing these parts, both in the case of the transmitter and the receiver.

2.3.1 Mixer

The mixer component is used to perform the frequency conversion. Mixers utilize non-linear devices such as diodes and transistors to perform their task. The component has three ports, where two of them are the inputs and one is the output. One of the inputs is used for a signal while the other input is used for an oscillator signal with a certain frequency. The mixer will output the initial signal at a frequency equal to that of its original frequency added to or subtracted from the frequency of the oscillator. The mixer works as a signal multiplier where the multiplication of the signals result in an addition in frequency. This is illustrated in equation 2.17 where an example of IF - RF conversion is presented.

$$\begin{aligned} v_{LO} &= \cos(2\pi f_{LO} t) \\ v_{IF} &= \cos(2\pi f_{IF} t) \\ v_{RF} = K v_{LO} v_{IF} &= K \cos(2\pi f_{LO} t) \cos(2\pi f_{IF} t) = \\ = \frac{K}{2} &[\cos(2\pi(f_{LO} - f_{IF})t) + \cos(2\pi(f_{LO} + f_{IF})t] \end{aligned} \tag{2.17}$$

In equation 2.17, K represents the voltage conversion loss through the mixer. It can be observed that the mixer will output an additional copy of the signal that has a frequency equal to the oscillator frequency subtracted by the initial signal's frequency. This frequency is referred to as the image frequency and is illustrated for the transmitter mixer in figure 2.8.

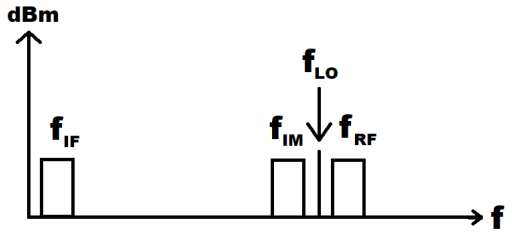

Figure 2.8: Illustration of the frequency conversion in the transmitter part of the block.

In figure 2.8, the signal with upper frequency is desired for communication, the oscillator signal and the image signal can be viewed as byproducts that can be filtered out. A dampened oscillator signal will be present on the mixer output due to imperfect isolation. Also, due to imperfect isolation, harmonics will be present at the mixer output. Harmonics are generated by the oscillator and are a result of non-linear components. Harmonics are located at frequencies that are a multiple of the oscillator's frequency, making them easy to filter out using band pass filters.

Like all microwave components, the mixer will affect the gain of the signal and contribute to the noise of the system. The mixer's effect on gain is called conversion loss since it is often negative, resulting in a dampening of the signal. Diode based mixers generally have a few decibels of conversion loss while transistor based mixers generally have a lesser conversion loss and possibly even a conversion gain[21].

2.3.2 Oscillator

An oscillator or a frequency synthesizer provides a narrow frequency signal that the mixer uses for frequency conversion. For this purpose, crystal oscillators are often used in combination with synthesizing techniques. Crystal oscillators are made from quartz and utilize the piezoelectric effect. Crystal oscillators generally have a high quality factor and provide high frequency stability. However, the resonant frequency of a crystal oscillator is generally in the megahertz regime and its frequency cannot be steered. Different synthesizing methods can be used to derive a range of higher frequencies from a crystal oscillator. The three main synthesizing methods are direct synthesis, PLL synthesis and digital synthesis.

Ideally, an oscillator should output a pure sinusoidal wave equivalent to a Dirac delta function in the frequency domain. However, due to phase noise, the output of an oscillator will have a small width with a gradual decline in the frequency domain. This is shown in figure 2.9.

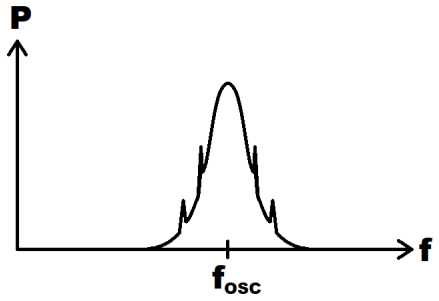

Figure 2.9: Illustration of a realistic output from an oscillator in the frequency domain.

Different noise sources in the frequency synthesizer will contribute to random fluctuations in phase, which takes the approximate shape of a normal distribution around the oscillation frequency in the frequency domain. In figure 2.9, small spikes are located on the slopes. These spikes are spurious frequency products that are a result of oscillator harmonics or mixing products from the different components in the synthesizer.

In the receiver part of this block, phase noise can lead to down-conversion of undesired signals that are located close to the desired signal in the frequency spectrum. These undesired signals will be down-converted to the IF band if the phase noise slope has power spectral density at a distance from the oscillator frequency that is equal to the distance between the desired and undesired signals. This will degrade the desired signal in the IF band. Phase noise will therefore limit how close signals can be located in the frequency spectrum. A sufficient guard band between the channels will negate these effects.

Phase noise is specified as the ratio of power between the phase noise slope at a specific offset from the oscillator frequency and the desired signal power, per hertz. Phase noise is often expressed in relation to the carrier power, giving phase noise the unit dBc/Hz. The requirement for phase noise can be calculated at a certain offset with respect to carrier power, signal suppression, undesired signal power and IF bandwidth[21]. The formula for this is given in equation 2.18.

$$\mathcal{L}(f_m) = C(dBm) - S(dB) - I(dBm) - 10log(B) \tag{2.18}$$

With the formula in equation 2.18, the phase noise requirement of a frequency synthesizer can be calculated based on channel spacing and adjacent channel rejection.

Controlling the frequency of an oscillator is useful when a communication system needs to switch between certain channels. By changing the frequency of the oscillator at the mixer input, different frequency channels can be tuned in by the communication system. A VCO is an oscillator where a voltage level is used to select the output frequency. This enables the transmitter to transmit on a specific channel while the receiver is able to receive on another channel by only changing the voltage levels at the input of the corresponding oscillators.

2.4 RF Beamforming Block

Beamforming is a frequently employed technique in modern communication systems, allowing the radiated energy from an antenna array to be concentrated in a specific, often steerable, direction. This in turn allows a better directivity leading to less interference between users, resulting in an overall higher signal quality. This does, however, come at the cost of additional complexity since there is a need for element specific phase and/or amplitude shifts. The complexity is further increased when the receiver is moving relative to the transmitter, as the transmission beam may need to change over time in order to continue using the optimum beam.
In an ideal beamformer, only a singular beam exists, allocating all radiated energy in the direction of the main lobe. This is, in reality, never the case and there is always some degree of side lobes as illustrated in figure 2.10. These side lobes utilize some of the available radiation energy, meaning the main lobe will have less power allocated to it. In addition to this, side lobes run the risk of interfering with other users, something which can in part be counteracted by null-forming.

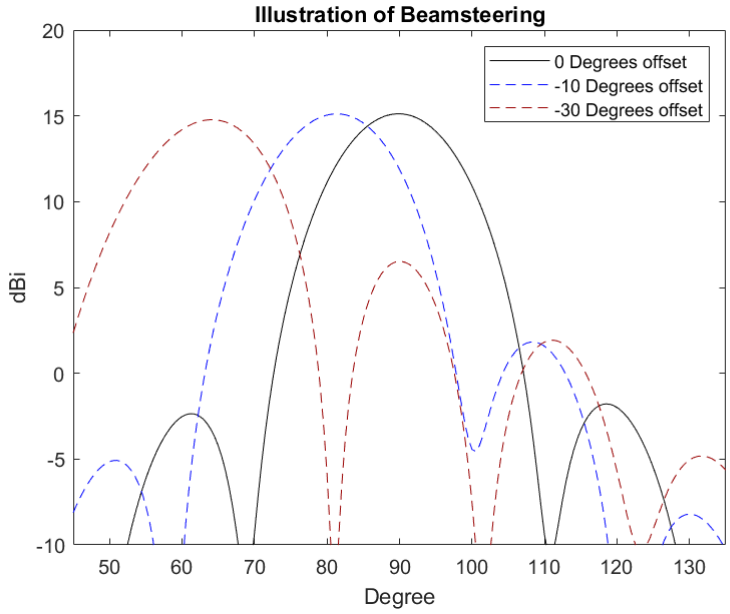

Figure 2.10: Example of beam steering. Here, the beam is steered with offsets from the initial main lobe at 90°.

2.4.1 Amplification Block

Some type of amplification for transmitted and received signals is an integral part of any communication system. Without it, communication systems would struggle to achieve high rate wireless communication, as the transmitter would be very limited in terms of transmittable signal power, while the receiver would struggle to distinguish the received signals from noise. This section primarily covers the amplification block presented in figure 3.1. Although, this section will also present relevant information for other blocks that use gain modification.

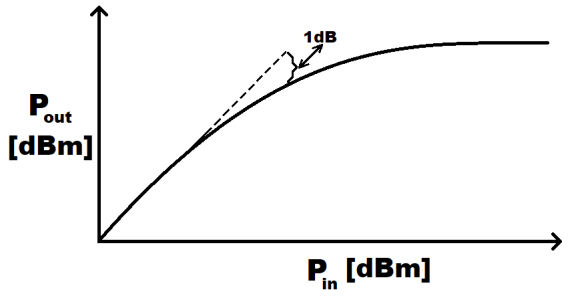

Figure 2.11: Illustration of the 1dB compression point.

Additionally, the OIP_3 is often specified, which is the point where the 3^{rd} order intermodulation product would have become larger than the intended signal if the input-output relationship was linear[22]. The level of the 3^{rd} order intermodulation distortion could possibly limit the performance of the system if these distortions become larger than the thermal noise of the system. The power level of the 3^{rd} order intermodulation distortion is calculated using the formula presented in 2.19.

$$P_{IM3,dBm} = 3 \cdot P_{out,dBm} - 2 \cdot OIP_{3,dBm} \tag{2.19}$$

It is especially important to consider the 3^{rd} order intermodulation distortion in the transmitter since communications standards often specify levels of allowed distortion in order to mitigate channel interference.
The amplifier, as all electrical components, will contribute thermal noise, increasing the overall noise level. This is often characterized in terms of a noise-figure, detailing how much noise the component incurs. Commonly, several amplifiers are cascaded in order to obtain sufficient gain. If such a setup is used, it is important to consider the fact that any noise which the first amplifier incurs will be amplified in the following stages[21]. A chain of cascaded components will have a total noise figure in accordance with the formula presented in equation 2.20, in linear units. For this reason, an LNA is often used as the first amplifier in the chain to keep the system's total noise figure as low as possible.

$$F_{tot} = F_1 + \frac{F_2 - 1}{G_1} + \frac{F_3 - 1}{G_1 \cdot G_2} + ... + \frac{F_n - 1}{G_1 \cdot G_2 \cdot ... \cdot G_{n-1}} \tag{2.20}$$

In equation 2.20, F_{tot} is the system's total noise figure, F_1 and G_1 is the noise figure and gain of the first component in the chain while F_n is the noise figure of the last component in the chain.
Contradictory to amplification, It is sometimes useful to use variable attenuation in order to make the system resilient against higher input power levels. Step attenuators are convenient to use as their attenuation is easily steered using the logical bits. Here, the sum of the logical bits multiplied with the step size will determine the attenuation. similarly, the step size along with the number of bits will determine the maximum available attenuation, the total available attenuation is presented in equation 2.21.

$$L_{max} = L_{step} \cdot (2^N - 1) \tag{2.21}$$

2.5 High Q-factor Filter Block

In order to band-limit the signal seen by the antenna, a filter is needed. Typically, filters incur some attenuation characterized by its insertion loss. They are also characterized by their center frequency and bandwidth, which describe the range of frequencies which the filter lets through. In terms of actually realizing filters, many different techniques exist which are suitable for different applications. Another parameter used for characterizing filters is the Q-factor which, roughly speaking, describes how fast the filter response transitions from pass-band to stop-band. In addition to filtering being utilized at the antenna, it can also be used in other blocks to suppress unwanted signals.

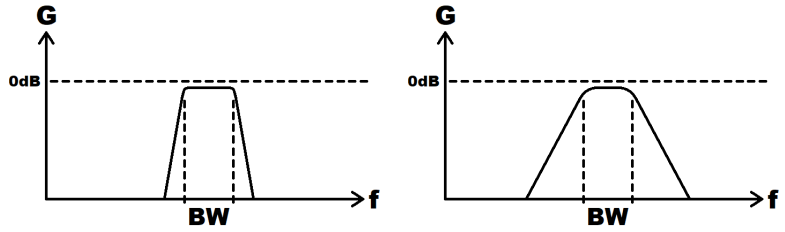

(a) High Q filter **(b)** Low Q filter

Figure 2.12: Examples of a) high Q filter and b) low Q filter.

2.6 Antenna Array Block

Some type of antenna is needed in order to transmit and receive a wireless signal. In order to utilize beamforming, multiple antenna elements are required, forming what is often referred to as an antenna array. For frequencies above 100 GHz, a slotted array antenna is one possible design. Slotted array antennas consist of wave guides that have slots through which the signal propagates. There are several ways of positioning these slots in the wave guides. If beamforming is applied for azimuth beam steering only, an intuitive design technique is vertical waveguides with lengthwise slots on one of the wider faces of the wave guide. These slots are positioned at an offset from the middle of the wider face, the sign of the offset is alternated between positive and negative for each slot. By having several slotted waveguides positioned next to each other, the array is formed. Here, the slots along the wave guides constitute one dimension of the array while the wave guide make up the other dimension[23][24].

2.7 Wireless channel

When communicating over a channel, any signal being transmitted is subject to noise. In the case of a wireless link, as for this project, multiple effects worsen the signal quality over the channel. The most obvious of these effects would be the

effects of path loss, meaning the transmitted signal loses some of its energy over the propagation path and can be modeled by equation 2.22[17]

$$L_{FS} = -10log_{10}(\left[\frac{\lambda}{4\pi d}\right]^2) = -10log_{10}(\left[\frac{c}{4\pi df}\right]^2) \tag{2.22}$$

where d is the distance between the communicating device antennas. In addition to the free-space path loss, shadowing occurs on any given wireless channel. Shadowing is the effect which objects blocking the LOS path has on the signal quality, along with some effects from multi path [17].
A model which includes the shadow-fading, as well as some environmental factors while also being valid for frequencies up to 100 GHz is the CI (close-in) model[25]. This model is presented in 2.23, where n (Path loss exponent) and SF (Shadow Fading) depend on the type of environment which the channel exists in. Although the model is claimed to be valid for frequencies up to 100 GHz it is valid even beyond that according to some sources [26][27].

$$L_{FSCI} = 20log_{10}(\frac{4\pi f}{c}) + 10nlog_{10}(\frac{d}{1m}) + SF \tag{2.23}$$

3
Method

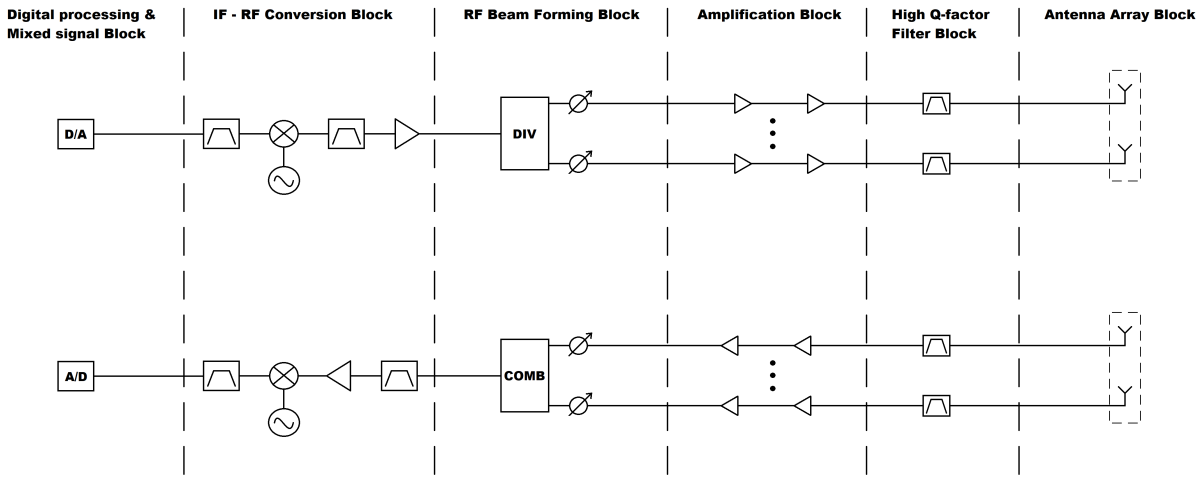

Figure 3.1: Illustration of the different blocks in the considered communication system.

During this project, a link budget analysis for a W-band communication system, along with some variations for it, has been conducted. These variations include the usage of a smaller antenna, a shared antenna and re-purposing the communication system to function as an FMCW radar. To simplify the analysis of said system variations, the general system overview seen in figure 3.1 has been used as a starting point in order to get a general understanding of each of the blocks and the different components associated with them. The knowledge gained from this analysis has then been used to construct the schematics of the different system variations. In addition to this, a table including the power budget, OIP3 and noise spectral density at each point of the system has been made. Close communication with each of the ENTRY100GHz collaboration partners has been used to collect information about each component. In the cases where a component is not developed by one of the collaborating partners, a review of the currently available hardware has been made in order to determine reasonable parameters for the component in question.
All parameters for the components have then been used in order to calculate the aforementioned performance metrics at each part of the system. Since component values are subject to change, a series `MATLAB` script has been written to calculate the performance metrics for each variation of the system. Because of this, changes made in the parameters of components are reflected in all the relevant stages of the system. Additionally, since the ENTRY100GHz collaboration stretches much further

compared to the time frame of this thesis, it allows the collaborating partners to use the scripts even after the conclusion of this thesis.
The IEEE Standard for High Data Rate Wireless Multi-Media Networks–Amendment 2: 100 Gb/s Wireless Switched Point-to-Point Physical Layer standard [28] has been used as an indicator for how the system is allowed to be used. This includes parameters such as spectral mask, allowable transmission power, modulation orders and much more. This standard is valid for much higher frequencies than those targeted in the context of this system. Since no standards on the targeted frequencies were found, the standard has been used to get a sense of what might be reasonable to expect from the developed system.
For this project, a rather simple model called the "close-in model" for estimation of the channel has been used. This is because channel estimation is a vast subject which could easily span the entirety of this thesis. By using this model, more time can be spent on other parts of the link budget, which is why this model was chosen.

4
System Description

This section contains the analysis of the general system architecture, divided into each of the blocks presented in figure 3.1. Each of the different blocks contain an analysis of the components associated with said block. Additionally, some demarcations, remarks and conclusions on the different components in these blocks are stated.

4.1 Digital Processing Block

This section will cover our assumptions and choices along with an analysis of each part of the digital processing block. For this project, the digital processing is assumed to be implemented as software. From a prototyping view, implementing the digital processing block as software would give it more flexibility and allow changes even after the prototype is finalized.

4.1.1 Channel Coding

Since coding is a vast subject and coding gain is dependent on many parts of the system, its gain effects will not be considered for the link-budget. It will, however, be taken into consideration when calculating the achievable rates. In doing so, the codes mentioned in [28] will be considered as possible coding schemes. More specifically, these codes include LDPC coding with rates of 14/15 (high-rate) and 11/15 (low-rate), as well as 224/240 RS code. Since 224/240 RS code and 14/15 LDPC code has the same code-rate and coding complexity as well as FEC capabilities not being considered for the throughput calculations, LDPC and RS codes will be assumed equal in performance. Because of this, only code rates of 14/15 and 11/15 will be considered for the throughput calculations.

4.1.2 Pulse shaping

In anticipation for higher-frequency communication, there is an ongoing drive for standardization to ensure well-functioning communication systems[7]. The first accepted standard[28] for frequencies between 252 GHz and 325 GHz specifies spectral masks to be adhered to during communication on these frequencies. Additionally, although no specific pulse shape is selected, this project assumes that 10% of the bandwidth is dedicated to a guard-band as to not interfere with other users, although this comes at a cost of achievable rates.

4.1.3 Synchronization

When it comes to the synchronization, carrier phase, carrier frequency and timing offsets need to be considered. Phase noise will distort the received symbols but will not be covered in the digital processing block since the negative effects can be heavily reduced by the choice of oscillator. Therefore, phase noise will be taken into account when determining suitable oscillator characteristics. Pilot symbols are assumed to be implemented to counteract the phase offset and reduce it to negligible levels. Digital frequency-locked loops are selected in order to minimize the carrier frequency offsets. Lastly, maximum likelihood based functions are used to choose the optimum sample position, which effectively mitigates the timing offset.

4.1.4 Modulation

For the purpose of this investigation, the modulation orders suggested in [28] will be used as a guideline, which are BPSK, QPSK, 8-PSK,8-APSK,16-QAM and 64-QAM. 64-QAM, however, is not studied as it is too error-prone for this specific application. The standard also specifies that the peak power should be no more than 10 mW.

In order to achieve communication with a reasonable quality, it will be assumed that an error-rate of 10^{-5} is sufficient, contrary to 10^{-7} in [28]. To determine the required SNR for such a bit error rate to hold, the `bertool`[29] in `MATLAB` is used to plot BER as a function of SNR per bit, $\frac{E_b}{N_0}$. For all of the constellations, with the exception of 8-APSK, theoretical BER as a function of $\frac{E_s}{N_0}$ is integrated into `bertool`[29]. For the purpose of plotting BER as a function of $\frac{E_s}{N_0}$ for 8-APSK, a simulation script based on the template in [30] was used. Here, the maximum number of errors was set to 500, while the maximum number of bits was set to 10^9 for each $\frac{E_b}{N_0}$ value, with SNR ranging from 0 to 30 dB with 0.1 dB increments. Because it is a simulation, the plot for 8-APSK is plotted as points in figure 2.2. In order to then obtain the BER as a function of SNR, $\frac{E_s}{N_0}$, the number of bits per symbol also has to be considered. This is taken into account by letting

$$E_b \cdot log_2(M) = E_s \tag{4.1}$$

the result of which can be seen in figure 2.2. Additionally, for constellations with more than 1 bit per symbol, a symbol error does not necessarily mean that all bits are in error, but rather that some bits are in error. The `bertool`[29] in `MATLAB` uses gray-mapping to calculate the error-rate, meaning as few bits as possible change for close-by mapping points[11]. This yields the error-rates seen in figure 2.2. Since `bertool` does not have an in-built function for theoretical BER for 8-APSK, a simulation script was written for it.

Using figure 2.2, it becomes clear that in order to achieve the aimed for BER of 10^{-5} with each modulation, an average SNR equal to that seen in table 4.1 is needed. In the table, E_s/N_0 is the signal to noise ratio, while E_b/N_0 is the energy per bit to noise ratio. The E_b is obtained using equation 4.1.

Modulation	E_s/N_0 [dB]	E_b/N_0 [dB]
BPSK	9.6	9.6
QPSK	12.6	9.6
8-PSK	17.7	12.9
8-APSK	16.7	11.9
16-QAM	19.4	13.4

Table 4.1: Minimum needed E_s/N_0 and E_b/N_0 for an error rate of 10^{-5} for the constellations considered.

The standard in [28] also puts some requirements on the EVM to allow the usage of the constellations in combination with some specific FEC-rates. These requirements can be seen in table 4.2. Since no prototype has been built for this project, no measurements can be carried out. Because of this, the EVM is used to verify whether or not the calculated non-linearities at the transmitter are small enough to be viable.

Modulation	Max EVM[dB]	FEC-rate
BPSK	-3	11/15
BPSK	-6	14/15
QPSK	-6	11/15
QPSK	-9	14/15
8-PSK	-11	11/15
8-PSK	-14	14/15
8-APSK	-11	11/15
8-APSK	-14	14/15
16-QAM	-13	11/15
16-QAM	-16	14/15

Table 4.2: suggested Requirements on EVM for specific modulation order and code rate[28]

4.1.5 Throughput of the system

For the specific system at hand, code rates of 11/15, 14/15 and 224/240 are possible[28]. Since 224/240 and 14/15 yield an equal code-rate, only 14/15 will be considered in the table.

A summary of the throughput upper bound for each modulation can be seen in table 4.3. The values in the table are calculated using equation 2.8. The table also contains the minimum peak-SNR needed in order to use each of the constellations with an error rate $< 10^{-5}$.

Modulation	Min SNR_{peak} [dB]	Throughput [Gbit/s] code rates [11/15 14/15]
BPSK	9.6	[3.3 4.2]
QPSK	12.6	[6.6 8.4]
8-PSK	17.7	[9.9 12.6]
8-APSK	18.8	[9.9 12.6]
16-QAM	22.0	[13.2 16.8]

Table 4.3: Throughput for different combinations of modulation order and code-rates [11/15, 14/15]. Here, BER is assumed to not impact the throughput, while frame overhead and back-off time is not considered either.

4.2 Mixed Signal Block

In order to sample or quantize the signal in a swift enough manner, the ADC needs a fast-enough clock. This puts some requirements on its speed for the selected ADC circuit. For the purpose of this work, a 3 dB bandwidth of 10% the entire bandwidth will be assumed. This means that in order to utilize the narrowest band available in [28], a sampling speed of $4.5 \times 2 \times 1.1 \approx 9.9$ GS/s is needed. while 9.9 GS/s is undoubtedly a tough requirement to meet, it is by no means impossible, as made evident in [31][32][33]. In order to meet this requirement, the ADC [20] is used as a reference for calculations. For this specific ADC, which samples at 10.25GS/s, $f_s = 5.125 \cdot 10^9$ Hz. Lastly, using equation 2.15 along with the sampling speed and Δ for the ADC, the PSD of the quantization noise becomes -144.2 dBm/Hz.

The ADC discretizes the analog input signal into a digital one. In doing so, some information is lost with regards to both time and amplitude. This will undoubtedly deteriorate the system performance by some amount, which for the purpose of this project needs to be a quantifiable amount. Similarly to other components in the hardware chain, this can be done using a noise figure estimation. Since the data sheet for the chosen ADC circuit [20] does not include this, some way of estimating it from some other parameters is needed. For this purpose, the formula presented in [34] is used, which can be seen in equation 4.2. Here, P_{FS} is the full-range input power for the ADC, B is the noise-bandwidth of the filter, here assumed to be 5 GHz and SNR is the SNR of the ADC. The ADC SNR is found in the data sheet [20] for the chosen ADC in this project. In the data sheet, SNR is specified for a few specific frequencies, as seen in table 4.4. The SNR value presented for 5 GHz is used despite the channel being only 4.5 GHz wide, in order to account for the noise bandwidth being wider than the actual filter bandwidth. Using equation 4.2 in conjunction with equation 4.3[34], where $R = 50\Omega$ is the input-impedance of the ADC and V_{pp} is the peak-to-peak voltage of the ADC to obtain $P_{FS} = 6.9$dBm, an SNR of 48 dB and a bandwidth of 5 GHz, the noise figure for the ADC can be estimated to 35.91dB.

$$NF = P_{FS} + 174 - SNR - 10log_{10}(B) \tag{4.2}$$

$$P_{FS} = \frac{(\frac{V_{pp}}{2})^2}{2R} \tag{4.3}$$

f_{in}	SNR
170 MHz	58.2 dB
1 GHz	56.8 dB
2.6 GHz	52.3 dB
4 GHz	50.2 dB
5 GHz	48 dB

Table 4.4: Table showing SNR as a function of input frequency. For 5 GHz, the value is extrapolated using the function polyfit in MATLAB.

The received power at the receiver cannot be assumed constant since a wireless channel is constantly changing. Because of this discrepancy in received power, there is the possibility that the ADC will experience input-powers less than the full range, meaning less bits will be used to perform quantization. This, in turn, reduces the SNR of the ADC, meaning its noise-figure will increase as can be seen in equation 4.2[35] and figure 4.1. The way which the NF is impacted can be derived by studying the number of bits utilized in the ADC quantizer, which is described in equation 4.4[35]. For the purpose of writing the number of used bits as a function of input-power, equation 4.5 is used. This in turn means that equation 4.4 can be re-written as equation 4.6. This can then be used to obtain equation 4.7[35], describing the SNR of the ADC as a function of bits used in the quantization, along with the thermal noise for the frequency which the ADC operates at. The thermal noise is obtained by comparing the SNR obtained from equation 4.7 while omitting thermal noise and the actually measured values in the data sheet [20].

$$b = n + log_2\left(\frac{V_{utilized}}{V_{Fullscale}}\right) \tag{4.4}$$

$$P_{rms} = \frac{(V_{rms})^2}{2R} \tag{4.5}$$

$$b = n + log_2\left(\sqrt{\frac{P_{in}}{P_{FS}}}\right) \tag{4.6}$$

$$SNR = 6.02b + 1.78 - N_{thermal} \tag{4.7}$$

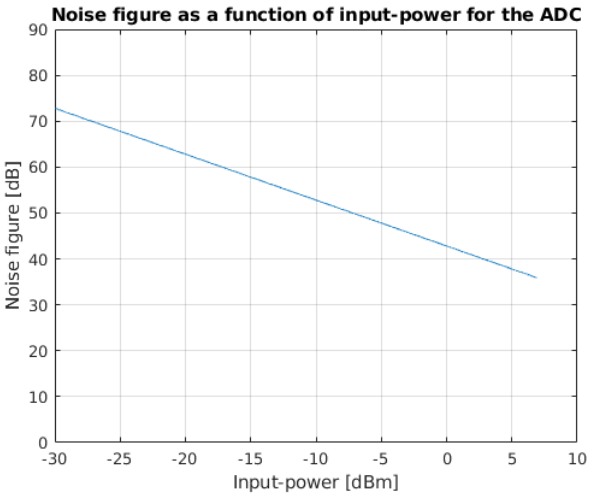

Figure 4.1: Noise figure of the ADC as a function of its input-power

As for the DAC used in this project, it is assumed that the DAC is able to output approximately -9 dBm at any frequency. However, the level is assumed to be adjustable to any power below -9dBm as well, in order to allow flexibility. It is also assumed that the output impedance of the DAC is 50 Ω.

4.3 IF - RF Conversion Block

4.3.1 Mixer

One interesting candidate for mixer designs above 100 GHz is Schottky diode based mixing. There are several proposed and realized mixers based on Schottky diodes that operate near 100 GHz[36][37][38]. These mixers have rather high conversion losses somewhere in the range of 5-15 decibels. However, these mixers provide a mixer bandwidth on the order of tens of gigahertz. For these reasons, a conversion loss of 10 dB for the mixers operating above 100 GHz is assumed.
In order to receive a specific channel, an intermediate mixing approach is chosen for this project. By steering the frequency at the input of the mixer operating above 100 GHz, the mixing of the incoming RF spectrum can be adjusted so that the desired channel is located at a fixed frequency interval in the X-band. After filtering, a X-band mixer can then be used to bring the desired channel to the IF frequency of the ADC. For the mixer operating on the lower frequency band, the conversion loss is assumed to be 7 dB.

4.3.2 Oscillator

For the purpose of this project, a VCO is used in the mixing stage of the transmitter so that the communication system is able to select the transmission band. The frequency of this VCO spans from 100 GHz to 115 GHz. Similarly, a VCO is used in the receiver to mix the desired signal to a specific frequency interval in the X-band which can then be filtered out. A fixed oscillator is then used to mix the signal in

the X-band down to the IF band. Here, the frequency of the VCO spans between 92.5 GHz and 107.5 GHz while the frequency of the fixed oscillator is 7.5 GHz.
As phase noise originates in the oscillators, there needs to be some limit in order for the system to be able to decode the signal. Using equation 2.18, the oscillators phase noise needs to be below -122 dBc/Hz if it is assumed that the interfering signal is as strong as the carrier and that the suppression should be 25 dB.

4.4 RF Beam forming Block

Due to interference not being considered for this work, nullforming technology is not taken into account. Beamforming, however, is accounted for in this work. It is further assumed that receivers are located within the main-lobe of the beamformer, meaning the system can reap its benefits. In order to achieve beamforming, the required dividers/combiners are based on waveguide structures developed within the ENTRY100GHZ collaboration. The phase shifters are also based on a design developed within the ENTRY100GHZ collaboration.

4.5 Amplification Block

The IEEE Standard for High Data Rate Wireless Multi-Media Networks standard[28] is used as reference for determining a reasonable allowed level of 3^{rd} order intermodulation distortion. With this in mind, a level of -25 dBc is determined to be a reasonable limit. Therefore, the transmitter should have a 3^{rd} order intermodulation distortion level below -25 dBc.
Power amplifiers are developed within the ENTRY100GHZ collaboration. For this reason, component values for the power amplifiers are chosen to reflect the performance of those developed within the collaboration. Similarly, component values for the LNAs are based on the LNA candidates considered by the partners of the ENTRY100GHZ collaboration. For the X-band amplifiers and variable attenuator, reasonable values based on currently available hardware was assumed.

4.6 High Q-factor Filter Block

Filters for the ENTRY100GHz collaboration are in development, although at the time of this work they are not presentable. Because of this, reasonable values based on filters for similar frequencies are used. When reviewing the available literature, it becomes evident that filters for the upper W-band indeed exist [39][40][41]. Such filters achieve insertion losses in the 3 dB range for tunable filters, while non-tunable filters seem to be able to achieve around 1 dB insertion loss. All of the filters achieve varying bandwidths, although the bandwidth is often on the order of one or a few percent of the center frequency. For the system at hand, utilizing a tunable filter which degrades the signal quality significantly more is likely a viable, although more challenging candidate. The previously mentioned 3 dB loss for a tunable filter will contribute an equally large noise figure, degrading the signal significantly more when

compared to a fixed filter, which incurs attenuation and noise figure on the order of 1 dB. For these reasons, a non-tunable filter will be used in this work.

Since non-tunable filters are to be used for the system at hand, some other way of isolating channels needs to be implemented. To realize this in practice, at least two filters are needed in the receiver. Firstly, a band-pass filter which lets through the entire band of interest is needed at the receive antenna to band-limit the signal, limiting the input-noise. To then separate channels within the band, a fixed band-pass filter with passband slightly larger than one channel bandwidth should be utilized. In order to then pick specific channels, the VCO which is connected to the mixer is steered such that the specific channel is down-mixed to IF-band. What has been described here is visualized in figure 4.2

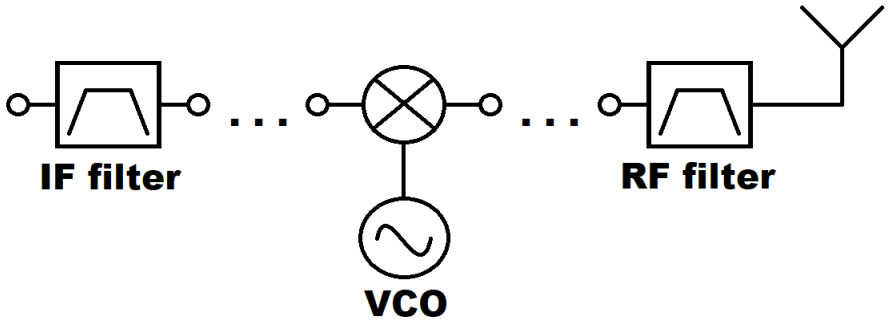

Figure 4.2: Illustration of placement of the filter block in the described system.

The filters themselves are also realized in different ways. The currently considered filters for frequencies around 100 GHz are of wave guide type. This is because a micro-strip filter at those frequencies would incur heavy losses. For filters in the range of 0 to 5 GHz, an off-the-shelf lumped-element micro-strip filter will be used due to low losses combined with ease of realization and cost effectiveness. However, in the range between 7.5 and 12.5 GHz, many options exist and no clear decision has been made. For the purpose of this work, filters within this range are assumed to be micro-strip based, for the sake of transitions.

4.7 Antenna Array Block

The main slot array antenna considered for this project is an 8-by-8 array, illustrated in figure 4.3. A similar antenna with only 4 columns containing 8 elements each is also considered as one of the variations of the system. This is because a smaller antenna simplifies the circuit layout compared to an 8 column one. This, however, has the drawback of decreasing the gain of the antenna by approximately 3 dB.

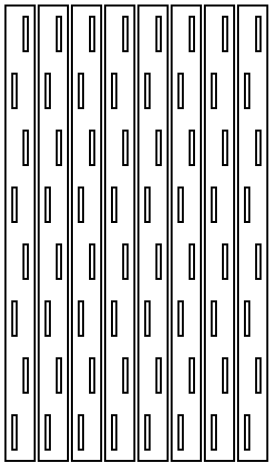

Figure 4.3: Graphical representation of an 8-by-8 slotted array antenna.

For the link budget calculation, the most important parameter of the antenna is the gain it provides. The gain of the antenna will be added twice to the link budget since the signal will be both transmitted and received by a similar antenna. Current simulations with the considered antenna show a gain between 18 and 23 dB (or 15-20dB for a similar 4-column antenna) is achievable with azimuth beam steering from 0 to 60 degrees, where 0 degrees correspond to the highest gain. Although the gain depends on frequency, it is assumed to hold for the entire RF band of 100-120 GHz for simplicity's sake.

4.8 Wireless channel

For the purpose of this work, the CI model presented in [25], seen in equation 2.23, will be utilized. To account for variations in channel losses due to the difference in frequencies, each channel will be assumed to experience the same loss as the center frequency in the respective channel, namely 102.5, 107.5, 112.5 and 117.5 GHz. This is in spite of the fact that the presented model is stated to hold for frequencies below 100 GHz. However, when a comparison between the computed loss and measurements done in [26][27] is made, it becomes clear that the model seems to agree fairly well even above the intended frequency range, a claim which is supported in [42]. for this reason, it will be used as an accurate-enough model for the intended system frequencies.
In addition to the discussed effects, wireless channels are plagued by interference from other users [17], although it will not be considered in this work. The reasoning behind this is that few applications of today transmit on this frequency band. Since few applications actually utilize the band, combined with its high path-loss in equation 2.23, it is unlikely to be subject to much interference from other users. However, even though interference from other users is not considered, it does not mean the system is allowed to transmit an arbitrary amount of energy. Instead, to

comply with interference requirements set in [28], a maximum output power of 10 dBm before the antenna will be used as a guideline.
In equation 2.23, SF is the shadow fading specified in [25], in this work assumed to be equal to one standard deviation for the specified case. For an urban micro cell with line of sight and an "open square" environment, SF=4.2 dB. n = 1.85 is the PLE for the same case, while f is the operating frequency and d is the separation between the Tx/Rx in meters. The reason for the division by one in the second term is to allow the usage of the same PLE presented in [25], as that is the reference distance used. This model does not consider antenna gain and it therefore needs to be taken into account separately. Using the described model, the losses which it incurs on the signal can be seen in figures 4.4 and 4.5a. From these figures, it becomes evident that the impact of the channel is heavily correlated with the distance from the receiver. What this means is that the dynamics of received signal power is large, putting strict requirements on the hardware design to account for these dynamics.

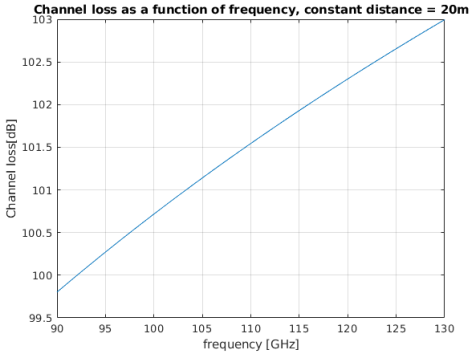

Figure 4.4: Channel loss as a function frequency for a constant distance d = 20 m

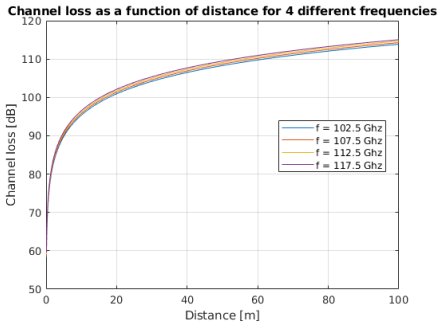

(a) Channel loss as a function of distance, 4 different frequencies

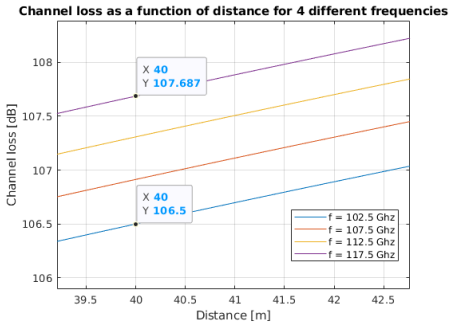

(b) Close-up of channel loss at distance of 40 m

Figure 4.5: Channel losses as a function of distance

5

System Investigations

5.1 Comparison Between Separate Modules and Switchable Module

For the system at hand, it will be assumed that an architecture where the transmitter and receiver have separate antennas are used. There is however the option of utilizing the same antenna for both transmission and reception. If a single antenna is used, it is possible that the device will become cheaper, assuming that the additional switches required are not more expensive than the antenna itself. The second large advantage with such a system is the possibility to utilize channel reciprocity[43]. Reciprocity is made possible for a single-antenna structure because the transmit- and receive-antennas then observe the same environment at any given point in time, since they are the same antenna. This allows the transmitter to use implicit feedback in order to estimate the channel meaning there will be less time required for channel estimation, allowing a lower overhead-rate for the communication link. Additionally, the channel being estimated starts at the same point in time as the receiver starts transmitting its channel estimation message, as opposed to when the transmitter sends its channel estimation frame to the receiver. In other words, the channel coherence time needs to fit one less frame compared to a non-reciprocal system in addition to less information needing to be transmitted. In addition to this, TDD allows the communication link to utilize a larger bandwidth in both up- and down-link as opposed to dividing the spectrum between the two, resulting in a possibly higher throughput in one direction if one of the communicating devices is assigned more transmission time. The additional bandwidth also allows the channel estimation message to be transmitted at a higher throughput compared to for example an FDD system, meaning the frame being sent occupies less time, leading to a longer available transmission time with an updated channel estimate.

The obvious drawback to a switched system is the fact that, since only one antenna is available, TDD will be required if duplex communication is to be achieved. While the usage of TDD in itself is not an objective drawback, the loss of flexibility and choice certainly is. Another major drawback is the impact which the switches have on the link-budget, with switches in such high frequency ranges incurring around 3-4 dB attenuation and a similar noise figure [44][45]. This, combined with the fact that more than one switch would be needed for such a system causes significant signal deterioration, especially on the receiver side where at least one of the switches would need to be put between the LNA and antenna, meaning its noise figure will have a significant impact on performance. Lastly, having a switched system means

there needs to exist some controlling of the actual switching, adding additional complexity. Also, in order to ensure reciprocity within the communication system, not only the wireless channel needs to be reciprocal but also the physical channel in terms of wave guides, amplifiers and so on. This can be largely accounted for using calibration, although this also adds some additional complexity. Depending on how the calibration is done, it may also require some additional information to be exchanged between the users [46]. The calibration, of course, requires some complexity in the form of computation power. Although an analysis of such aspects is outside the scope of this work, one has to consider such effects on the overall system complexity and the additional hardware requirements which it incurs.
If instead a structure with separate receiver and transmitter antennas is used, no additional switches will be needed, leading to a higher signal quality. This in turn may allow higher modulation orders while still fulfilling the BER-requirements set in [28], leading to a higher throughput. However, depending on the coherence time of the channel, it may still not lead to an increased information-throughput due to the higher degree of overhead associated with such a system. The additional overhead comes from at least one additional frame containing channel estimation and feedback needs to be sent from the second to the first user, while the first user then needs to send its feedback to the first user. The benefit with this setup is the possibility to utilize separate channels at once, enabling full-duplex communication. If the separate channels are assumed to be as wide as the TDD case, it also means that the users do not need to wait for each other before transmitting.

5.2 Interfaces Between The Different Blocks

There needs to be some transitions between micro-strip and waveguide, as well as vice versa for the studied system. This transition incurs some attenuation, on the order of 0.2 dB per transition for the currently developed ones. Because of this loss it is beneficial to include as few transitions as possible. However, one also has to consider the possibility of less attenuation if for example a waveguide filter is used instead of a micro-strip one for higher frequencies, as waveguide based components are often more viable for such frequencies.
The currently considered filters in the 100 GHz range consist of waveguide filters. Due to this, the signal must enter the filter via a waveguide. On the other hand, most other components are micro-strip based, meaning the signal must enter through a micro-strip connection. The transitions will effectively make up for this difference, allowing waveguide-based components to function properly in the same system as ones based on micro-strip.
For the receiver, the first transition from waveguide to micro-strip occurs after the RF-filter by the antenna. Here, the signal needs to go from waveguide to micro-strip in order to perform amplification on the received signal. The second transition is then needed before the combiner since the signals coming from the variable phase shifters propagate through a micro-strip, while the combiner requires a waveguide input. The waveguide filter after the combiner is followed by a power amplifier, meaning a third and last transition is needed from waveguide to micro-strip. In total, these transitions will incur a 0.6 dB loss between receiving the signal and

sampling it at the A/D converter.

On the transmitter side, the signal can propagate on a micro-strip until the first high-frequency filter right before the power amplifier. However, since power amplifiers need a micro-strip input, a second transition is needed right after the waveguide filter. The power divider, which operates on waveguide signals, then requires a third transition from micro-strip to waveguide. The phase shifter, which is the first component after the power divider, requires a fourth transition to micro-strip. Lastly, the filter and antenna operates on waveguide signals, meaning a fifth and last transition from micro-strip to waveguide is needed before those. All-in-all, these five transitions incur a 1 dB loss in signal power.

5.3 Different Requirements For Communication And FMCW Radar Systems

A FMCW radar system is strikingly similar component wise to a communication system. Both systems transmit and receive electromagnetic waves which require microwave components connected in a certain sequence in order for the systems to function properly. The main difference between a communication system and a FMCW radar system is what is transmitted and received by the respective systems. While the communication system transmits and receives information-bearing waves, the FMCW radar system transmits a single continuous frequency modulated wave. By changing a few components in the system chain, a communication system can be repurposed to a FMCW radar system.

As stated previously, a FMCW radar system uses a frequency modulated continuous wave for transmission. The frequency of the wave is modulated to linearly increase with time during the span of a chirp period, after which it resets to the frequency it had at the beginning. The frequency range of the sweep is referred to as the bandwidth. A VCO feed with either an analog voltage ramp generator or a digitally synthesized voltage ramp is generally used to modulate the continuous wave used for transmission. The power of the wave is however split before it is used for transmission, where half of the power is amplified and used for transmission and half of the power is used in the receiver.

The continuous wave is picked up by the receiver after it has propagated to and back from the target. After amplification, the received wave is mixed with the split transmission wave. Due to the time delay, there will be a frequency difference between the received wave and transmitted wave. Therefore, the mixing will produce a peak equal to the frequency difference between the signals. This is illustrated in figure 5.1.

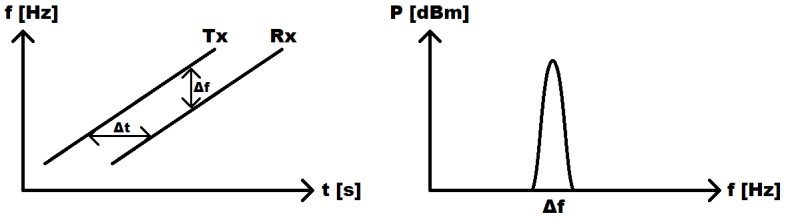

Figure 5.1: On the left, frequency of the transmitted and received waves with respect to time. On the right, The resulting frequency peak after mixing the transmitted and received waves.

Since the frequency is swept over a certain bandwidth in a certain time period, the slope of the transmitted and received waves in figure 5.1 will be equal to the bandwidth divided by the chirp period. Here, the time and frequency differences between the transmitted and received waves will form a 90° triangle with the same slope as the triangle formed by the bandwidth and the chirp period, as shown in equation 5.1.

$$S = \frac{B}{t_p} = \frac{\Delta f}{\Delta t} \tag{5.1}$$

Since the time delay is caused by the transmitted wave propagating to and back from a certain target, the time delay can be expressed as in equation 5.2.

$$\delta t = \frac{2R}{c} \tag{5.2}$$

With this in mind, the range to a certain target can be written as a function of the frequency difference the target causes, as shown in equation 5.3.

$$\frac{B}{t_p} = \frac{c\Delta f}{2R} \Longrightarrow R = \frac{ct_p\Delta f}{2B} \tag{5.3}$$

For multiple targets, multiple frequency peaks will appear in the received spectrum. These peaks need to have some separation to distinguish them from one another. For FMCW radar systems with a time bandwidth product larger than 10, the Reyleigh range resolution can be expressed by equation 5.4[47]. This represents the distance two objects must be separated in range for the FMCW radar system to be able to tell them apart.

$$\delta_R = \frac{c}{2B} \tag{5.4}$$

The maximum distance a FMCW radar system can detect a target is dependent on the sample frequency. This is due to the fact that the observed range of a certain target is proportional to the frequency peak generated by said target. Therefore, the maximum range will correspond to the maximum frequency the ADC is able to sample, which is half its sample rate. The maximum range can then be deduced by calculating the range of the maximum frequency peak, presented in equation 5.5. However, a quadrature demodulator contains two ADCs, which makes it able to sample frequencies up to the sample frequency. Therefore, if a quadrature demodulator

is used, the maximum range will instead be twice as large when compared to the case of a single ADC. The maximum range when using a quadrature demodulator is shown is equation 5.6.

$$R_{Max} = \frac{ct_p(0,5 \cdot f_s)}{2B} \tag{5.5}$$

$$R_{Max,Quadrature} = \frac{ct_p f_s}{2B} \tag{5.6}$$

By observing the linear phase change of the target frequency peaks between the chirps, the Doppler shift can be deduced. This is achieved by performing a Fourier transform across the chirps. The radial velocity can then be determined from the Doppler shift as the velocity is proportional to the Doppler shift. The formula for the Doppler shift is shown in equation 5.7.

$$f_D = \frac{2v}{\lambda} \tag{5.7}$$

Since the chirps are repeated each chirp period, the phase change of the target frequency peaks between the different chirps can be sampled at a rate equal to one divided by the chirp period. The maximum Doppler shift that can be sampled is limited by the Nyquist criterion, resulting in a maximum Doppler shift of half the Doppler sample rate. The maximum unambiguous velocity is achieved with the maximum Doppler shift, as shown in equation 5.8.

$$f_{D,Max} = \frac{1}{2t_p} = \frac{2v_u}{\lambda} \Longrightarrow v_u = \frac{\lambda}{4t_p} \tag{5.8}$$

The velocity resolution will correspond to the width of the Doppler shift peaks resulting from the Fourier transform between the chirps. The width of the Doppler shift peaks in frequency units is equal to the inverse of the coherent processing interval. The coherent processing interval is in turn equal to the chirp period multiplied with the number of chirps included in the Fourier transform across the chirps. The width of the Doppler shift peaks in frequency can be used to determine the resolution in velocity by using the relation between the Doppler shift and velocity, presented in equation 5.7. This results in a formula for the velocity resolution, presented in equation 5.9.

$$\delta f = \frac{1}{CPI} = \frac{1}{t_p N_{Chirps}} \Longrightarrow \delta v = \frac{\lambda}{2t_p N_{Chirps}} \tag{5.9}$$

A sufficient signal-to-noise ratio is needed to distinguish possible targets from the noise. The signal noise levels of a FMCW radar system will differ from a conventional communication system as these systems do not operate on the same principals. For a FMCW system, the transmitted wave will propagate to the target, then scatter and reflect back towards the receiver. This results in a propagation loss that is dependent on the radar cross section of the target and the distance to the target to the fourth power. The propagation loss is given in equation 5.10.

$$L_{Propagation} = \frac{(4\pi)^3 R^4}{\sigma \lambda^2} \tag{5.10}$$

in equation 5.10, σ is the radar cross-section.
Optimum signal processing will improve the noise level of a FMCW radar system with a factor equal to the time-bandwidth product. Furthermore, the noise level will be averaged by the number of chirps in the coherent processing interval. This gives a final noise level shown in equation 5.11.

$$N = \frac{N_0}{t_p N_{Chirps}} \tag{5.11}$$

FMCW radar systems are frequently used in automotive applications. This is partly due to the possible range and velocity resolutions these systems provide. The FMCW radar system considered in this project will be designed for automotive use.
For the velocity measurements, the FMCW radar system should be able to measure velocities up to about 200 km/h with an accuracy of 3,6 km/h. The chirp period is decided by the maximum unambiguous velocity as shown in equation 5.8. A chirp period of 13,2 μs is selected for a sufficiently high maximum unambiguous velocity. As shown in equation 5.9, the velocity resolution depends on the chirp period and the number of chirps. Since the chirp period is determined, the number of chirps is the deciding factor. The number of chirps is set to 110 to acquire a velocity resolution that complies with the previously stated criterion.
When it comes to the range measurements, the FMCW radar system should have a maximum detection range of more than 100 meters. Assuming that the FMCW radar used a quadrature demodulator, equation 5.6 shows how high the sampling frequency must be in order to obtain a specific maximum detection range. A sweep bandwidth of 500 MHz and a sampling frequency of 100 MHz gives a maximum detection range of 198 meters which is more than enough for the intended application. As shown in equation 5.4, the range resolution is decided by the bandwidth. A sweep bandwidth of 500 MHz results in a range resolution of 0.3 meters which is sufficient for the intended application. The filter bandwidth of the bandpass filters in the receiver are adjusted to account for the generated frequency peaks corresponding to the minimum and maximum range criteria. This puts the pass-band filters between 0.2 and 50 MHz.
At last, targets at different ranges will generate peaks with different signal-to-noise ratios based on said range. Therefore, the signal power and the noise power (including distortion) at the input of the demodulator are simulated as a function of range. A value for the radar cross-section of a generic target is needed for calculating the propagation loss. Since this application intends to detect cars at a longer range in traffic, it is most likely that the detected cars will be detected from either the front or the back due to the general flow of traffic. Measurements show that a radar cross-section of 10 m^2 is a reasonable assumption for detecting cars from the front and back[48]. Using this, the signal and noise power levels can be simulated as a function of range. A signal-to-noise level of 10 dB is determined as the limit of when a target can be distinguished from the noise. The signal-to-noise level will effectively limit the minimum and maximum target range of the FMCW radar system. At smaller ranges, the signal power in the receiver components will be too high, leading to both clipping and a distortion dominated noise level. At larger ranges, the signal level will be too low to achieve a sufficiently good signal-to-noise ratio. This creates the

need for a minimum detection range as this kind of limit has not been set. A range of 1 meter is determined to be a reasonable minimum detection range. The lower ranges are limited by the intermodulation distortion which becomes too high for a sufficient signal-to-noise ratio. By removing one amplifier in the transmitter and instead adding one in the very end of the receiver, the intermodulation distortion levels become low enough to achieve a sufficient signal-to-noise ratio at the 1 meter range.

6
Results

All of the mentioned effects in this paper culminate to a link budget for the system in development. In short, the link budget consists of signal power, noise spectral density and OIP3 which all combine to determine the performance of the system at both the receiver and transmitter. These parameters are summed up in tables 6.1 and 6.2, where each of the parameters are shown after every stage. As can be seen in figure 6.2, the system has an acceptable performance of at least 10 dB SNR between roughly -80 and -60 dBm input power at the antenna. When considering the output power and antenna gain at the receiver, this means the system is functional at a distance of approximately 3.8-45.1 m. If the devices are closer than that, the high input power will mean the non-linearities of the components at the receiver will deteriorate the signal quality too much to obtain a reasonable SNR value. If the distance is larger than 45.1 m, the thermal noise of the components will limit the performance. These effects are clearly visible in figure 6.2, where the SNR is increasing until the input-power is approximately 67.5 dBm, at which point the SNR decreases with input power, indicating that the non-linearities become the dominant term for the noise. In table 6.4 an overview of the system performance detailing the maximally achievable throughput for specific range and code-rate combinations can be seen. Here, it is seen that the highest usable modulation is 8-PSK if a BER of 10^{-5} is assumed. The table also details the highest achievable throughput for these cases when overhead and bit errors are excluded. It should be noted that in figure 6.2, the signal power is a description of the *average* transmit power. Since 16-QAM and 8-APSK are not constant-envelope constellations, their PAPR is added to the needed average SNR to remain comparable with the constant-envelope constellations.

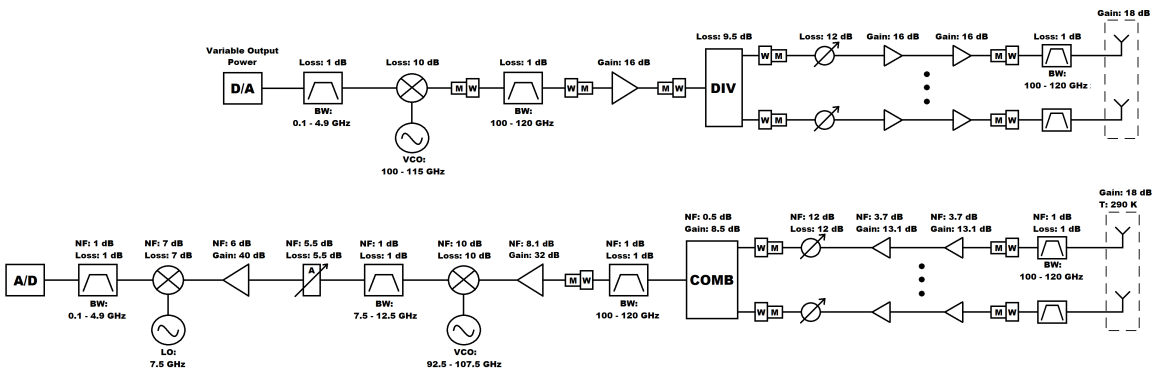

Figure 6.1: Block diagram of the examined communication system

Component	Power budget[dBm] f_c = [102.5,107.5,112.5,117.5] GHz	OIP3 [dBm] f_c = [102.5,107.5,112.5,117.5] GHz	Comment
D/A converter	[-12.7,-7.6,-10.0,-5.5]	-	
Filter 0.1-4.9 GHz	[-13.7,-8.6,-11.0,-6.5]	-	
Mixer 100-115 GHz	[-23.7,-18.6,-21.0,-16.5]	[16.0,14.0,12.0,10.0]	
Patch transition	[-23.9,-18.8,-21.2,-16.7]	[15.8,13.8,11.8,9.8]	Microstrip to waveguide
Filter 100-120 GHz	[-24.9,-19.8,-22.2,-17.7]	[14.8,12.8,10.8,8.8]	
E-plane transition	[-25.1,-20.0,-22.4,-17.9]	[14.6,12.6,10.6,8.6]	Waveguide to microstrip
Power amplifier	[-8.7,-4.3,-5.9,-2.9]	[26.6,25.8,24.5,22.1]	
Patch transition	[-8.9,-4.5,-6.1,-3.1]	[26.4,25.6,24.3,21.9]	Microstrip to waveguide
Power divider	[-18.4,-14.0,-15.6,-12.6]	[16.8,16.1,14.8,12.4]	
E-plane transition	[-18.6,-14.2,-15.8,-12.8]	[16.6,15.9,14.6,12.2]	Waveguide to microstrip
Phase shifter	[-30.6,-29.2,-30.8,-27.8]	[4.4,0.8,-0.5,-2.9]	
Power amplifier	[-14.2,-13.5,-14.3,-12.8]	[20.1,16.2,15.7,12.0]	
Power amplifier	[2.2,2.2,2.2,2.2]	[27.9,27.5,26.6,24.2]	
Patch transition	[2.0,2.0,2.0,2.0]	[27.7,27.3,26.4,24.0]	Microstrip to waveguide
Filter 100-120 GHz	[1.0,1.0,1.0,1.0]	[26.7,26.3,25.4,23.0]	
Antenna array	**[28.0,28.0,28.0,28.0]**	**[53.7,53.4,52.4,50.1]**	**EIRP**

Table 6.1: Transmitter power and OIP3 budget for frequencies [102.5, 107.5, 112.5 117.5] GHz, referred to output

Component	Power budget[dBm] f_c = [102.5,107.5,112.5,117.5] GHz	Noise spectral density [dBm/Hz] f_c = [102.5,107.5,112.5,117.5] GHz	OIP3 [dBm] f_c = [102.5,107.5,112.5,117.5] GHz	Comment
Received signal power	[-72.9,-73.3,-73.7,-74.1]	-	-	
Antenna array	[-64.0,-64.4,-64.8,-65.1]	[-174.0,-174.0,-174.0,-174.0]	-	
Filter 100-120 GHz	[-65.0,-65.4,-65.8,-66.1]	[-174.0,-174.0,-174.0,-174.0]	-	
E-plane transition	[-65.2,-65.6,-66.0,-66.3]	[-174.0,-174.0,-174.0,-174.0]	-	Waveguide to microstrip
LNA	[-52.1,-52.5,-52.9,-53.2]	[-157.2,-157.2,-157.2,-157.2]	[22.8,22.8,22.8,22.8]	
LNA	[-39.0,-39.4,-39.8,-40.1]	[-144.0,-144.0,-144.0,-144.0]	[22.6,22.6,22.6,22.6]	
Phase shifter	[-51.0,-54.4,-54.8,-55.1]	[-155.9,-158.8,-158.8,-158.8]	[9.9,6.9,6.9,6.9]	
Patch transition	[-51.2,-54.6,-55.0,-55.3]	[-156.1,-159.0,-159.0,-159.0]	[9.7,6.7,6.7,6.7]	Microstrip to waveguide
Combiner	[-42.6,-46.0,-46.4,-46.8]	[-156.6,-159.5,-159.5,-159.5]	[18.2,15.2,15.2,15.2]	
Filter 100-120 GHz	[-43.6,-47.0,-47.4,-47.8]	[-157.6,-160.5,-160.5,-160.5]	[17.2,14.2,14.2,14.2]	
E-plane transition	[-43.8,-47.2,-47.6,-48.0]	[-157.8,-160.7,-160.7,-160.7]	[17.0,14.0,14.0,14.0]	Waveguide to microstrip
Gain stage	[-11.0,-15.8,-14.6,-18.0]	[-124.4,-128.3,-126.7,-129.7]	[28.4,29.3,27.9,27.3]	
Mixer 92.5-107.5 GHz	[-21.0,-25.8,-24.6,-28.0]	[-134.4,-138.3,-136.7,-139.7]	[14.0,12.9,11.0,9.3]	
Filter 7.5-12.5 GHz	[-22.0,-26.8,-25.6,-29.0]	[-135.4,-139.3,-137.7,-140.7]	[13.0,11.9,10.0,8.3]	
Attenuator	[-27.5,-32.3,-31.1,-34.5]	[-140.9,-144.8,-143.2,-146.2]	[7.5,6.4,4.5,2.8]	Equalize amplitude to achieve full range of A/D
Two power amplifiers	[12.5,7.7,8.9,5.5]	[-100.9,-104.8,-103.2,-106.1]	[38.4,38.2,37.9,37.4]	
Mixer 7.5-12.5 GHz	[5.5,0.7,1.9,-1.5]	[-107.9,-111.8,-110.2,-113.1]	[24.1,24.1,24.0,23.9]	
Filter 0.1-4.9 GHz	[4.5,-0.3,0.9,-2.5]	[-108.9,-112.8,-111.2,-114.1]	[23.1,23.1,23.0,22.9]	
A/D converter	**[4.5,-0.3,0.9,-2.5]**	**[-108.9,-112.7,-111.1,-114.0]**	**[23.1,23.1,23.0,22.9]**	

Table 6.2: Receiver power budget, Noise density and OIP3 at every stage of receiver for frequencies [102.5, 107.5, 112.5 117.5] GHz and a distance of 20 m, referred to output

Parameter	Value f_c = [102.5, 107.5, 112.5, 117.5] GHz
Transmitter third-order intermodulation product level	[-51.4,-50.7,-48.9,-44.1] dBc
Noise Level	[-12.1,-15.9,-14.3,-17.2] dBm
Receiver third-order intermodulation product level	[-37.3,-46.8,-44.3,-50.9] dBc
Signal-to-noise ratio	[16.6,15.5,15.2,14.7] dB

Table 6.3: Performance parameters for frequencies [102.5, 107.5, 112.5 117.5] GHz at a distance of 20 m, referred to output

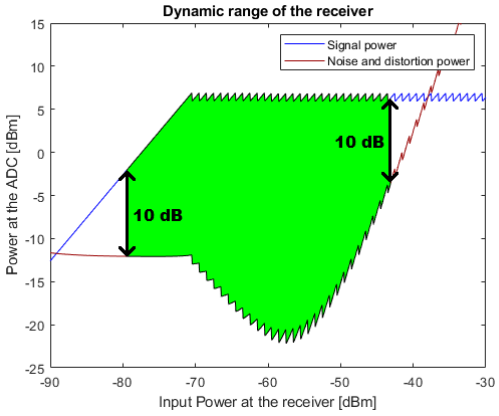

Figure 6.2: Dynamic input range of the receiver

Modulation	Min SNR_{peak}	Range [m]	Throughput [Gbit/s] code rates [11/15 14/15]
BPSK	9.6	0.5 - 47.3	[3.3 4.2]
QPSK	12.6	0.6 - 32.6	[6.6 8.4]
8-PSK	17.7	0.8 - 17.2	[9.9 12.6]
8-APSK	18.8	0.9 - 14.7	[9.9 12.6]
16-QAM	22.0	1.2 - 9.8	[13.2 16.8]

Table 6.4: Throughput for different combinations of modulation order and code-rates [11/15 14/15]

6.1 Variations of conditions

While analyzing the performance of the communication system at hand, there have been some requests of a performance analysis for a system with different conditions compared to the original case. The analysis of some of them have been conducted in a similar way to the original case. These cases and their link-analysis are presented below, along with their implications on performance.

6.1.1 4 column antenna

For this case, the antennas fitted on both the transmitter and receiver have 4 columns instead of the original 8. This halves the number of antenna elements on each side, limiting the achievable antenna gain by approximately half. The reason for including this case is the fact that a smaller antenna is allegedly, from a circuitry point of view, easier to implement. It also has the obvious benefit of being smaller than the 8 column antenna case.

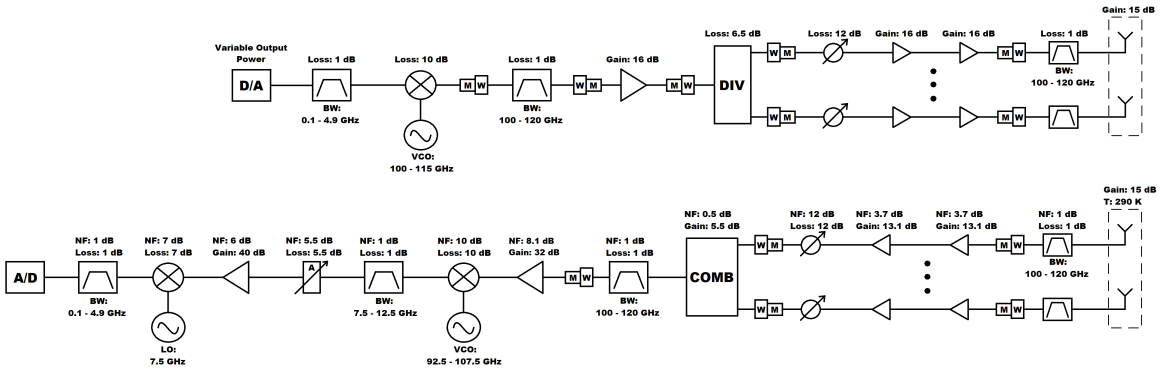

Figure 6.3: Block diagram of the examined 4 column antenna communication system.

Component	Power budget[dBm] f_c = [102.5,107.5,112.5,117.5] GHz	OIP3 [dBm] f_c = [102.5,107.5,112.5,117.5] GHz	Comment
D/A converter	[-12.7,-7.6,-10.0,-5.5]	-	
Filter 0.1-4.9 GHz	[-13.7,-8.6,-11.0,-6.5]	-	
Mixer 100-115 GHz	[-23.7,-18.6,-21.0,-16.5]	[16.0,14.0,12.0,10.0]	
Patch transition	[-23.9,-18.8,-21.2,-16.7]	[15.8,13.8,11.8,9.8]	Microstrip to waveguide
Filter 100-120 GHz	[-24.9,-19.8,-22.2,-17.7]	[14.8,12.8,10.8,8.8]	
E-plane transition	[-25.1,-20.0,-22.4,-17.9]	[14.6,12.6,10.6,8.6]	Waveguide to microstrip
Power amplifier	[-8.7,-4.3,-5.9,-2.9]	[26.6,25.8,24.5,22.1]	
Patch transition	[-8.9,-4.5,-6.1,-3.1]	[26.4,25.6,24.3,21.9]	Microstrip to waveguide
Power divider	[-15.4,-11.0,-12.6,-9.6]	[19.8,19.1,17.8,15.4]	
E-plane transition	[-15.6,-11.2,-12.8,-9.8]	[19.6,18.9,17.6,15.2]	Waveguide to microstrip
Phase shifter	[-27.6,-26.2,-27.8,-24.8]	[7.3,3.6,2.4,0.1]	
Power amplifier	[-11.2,-10.5,-11.3,-9.8]	[22.4,18.9,18.4,14.8]	
Power amplifier	[5.2,5.2,5.2,5.2]	[28.1,28.3,27.2,25.5]	
Patch transition	[5.0,5.0,5.0,5.0]	[27.9,28.1,27.0,25.3]	Microstrip to waveguide
Filter 100-120 GHz	[4.0,4.0,4.0,4.0]	[26.9,27.1,26.0,24.3]	
Antenna array	**[25.0,25.0,25.0,25.0]**	**[47.9,48.2,47.0,45.3]**	**EIRP**

Table 6.5: Transmitter power and OIP3 budget for frequencies [102.5, 107.5, 112.5 117.5] GHz, referred to output for the 4-column antenna case

Component	Power budget[dBm] f_c = [102.5,107.5,112.5,117.5] GHz	Noise spectral density [dBm/Hz] f_c = [102.5,107.5,112.5,117.5] GHz	OIP3 [dBm] f_c = [102.5,107.5,112.5,117.5] GHz	Comment
Received signal power	[-75.9,-76.3,-76.7,-77.1]	-	-	
Antenna array	[-67.0,-67.4,-67.8,-68.1]	[-174.0,-174.0,-174.0,-174.0]	-	
Filter 100-120 GHz	[-68.0,-68.4,-68.8,-69.1]	[-174.0,-174.0,-174.0,-174.0]	-	
E-plane transition	[-68.2,-68.6,-69.0,-69.3]	[-174.0,-174.0,-174.0,-174.0]	-	Waveguide to microstrip
LNA	[-55.1,-55.5,-55.9,-56.2]	[-157.2,-157.2,-157.2,-157.2]	[22.8,22.8,22.8,22.8]	
LNA	[-42.0,-42.4,-42.8,-43.1]	[-144.0,-144.0,-144.0,-144.0]	[22.6,22.6,22.6,22.6]	
Phase shifter	[-54.0,-57.4,-57.8,-58.1]	[-155.9,-158.8,-158.8,-158.8]	[9.9,6.9,6.9,6.9]	
Patch transition	[-54.2,-57.6,-58.0,-58.3]	[-156.1,-159.0,-159.0,-159.0]	[9.7,6.7,6.7,6.7]	Microstrip to waveguide
Combiner	[-48.6,-52.0,-52.4,-52.8]	[-156.6,-159.5,-159.5,-159.5]	[15.2,12.2,12.2,12.2]	
Filter 100-120 GHz	[-49.6,-53.0,-53.4,-53.8]	[-157.6,-160.5,-160.5,-160.5]	[14.2,11.2,11.2,11.2]	
E-plane transition	[-49.8,-53.2,-53.6,-54.0]	[-157.8,-160.7,-160.7,-160.7]	[14.0,11.0,11.0,11.0]	Waveguide to microstrip
Gain stage	[-17.0,-21.8,-20.6,-24.0]	[-124.4,-128.3,-126.7,-129.7]	[28.3,29.2,27.8,27.2]	
Mixer 92.5-107.5 GHz	[-27.0,-31.8,-30.6,-34.0]	[-134.4,-138.3,-136.7,-139.7]	[14.0,12.8,11.0,9.2]	
Filter 7.5-12.5 GHz	[-28.0,-32.8,-31.6,-35.0]	[-135.4,-139.3,-137.7,-140.7]	[13.0,11.8,10.0,8.2]	
Attenuator	[-33.5,-38.3,-37.1,-40.5]	[-140.9,-144.8,-143.2,-146.2]	[7.5,6.3,4.5,2.7]	Equalize amplitude to achieve full range of A/D
Two power amplifiers	[6.5,1.7,2.9,-0.5]	[-100.9,-104.8,-103.2,-106.1]	[38.4,38.2,37.9,37.4]	
Mixer 7.5-12.5 GHz	[-0.5,-5.3,-4.1,-7.5]	[-107.9,-111.8,-110.2,-113.1]	[24.1,24.1,24.0,23.9]	
Filter 0.1-4.9 GHz	[-1.5,-6.3,-5.1,-8.5]	[-108.9,-112.8,-111.2,-114.1]	[23.1,23.1,23.0,22.9]	
A/D converter	**[-1.5,-6.3,-5.1,-8.5]**	**[-108.9,-112.5,-111.0,-113.6]**	**[23.1,23.1,23.0,22.9]**	

Table 6.6: Receiver power budget, Noise density and OIP3 at every stage of receiver for frequencies [102.5, 107.5, 112.5 117.5] GHz and a distance of 20 m, referred to output for the 4-column antenna case

Parameter	Value f_c = [102.5 107.5 112.5 117.5] GHz
Transmitter third-order intermodulation product level	[-45.9,-46.3,-44,-40.6] dBc
Noise Level	[-12.1,-15.7,-14.2,-16.8] dBm
Receiver third-order intermodulation product level	[-49.3,-58.8,-56.3,-62.9] dBc
Signal-to-noise ratio	[10.5,9.3,9.1,8.2] dB

Table 6.7: Performance parameters for frequencies [102.5, 107.5, 112.5 117.5] GHz at a distance of 20 m, referred to output for the 4-column antenna case

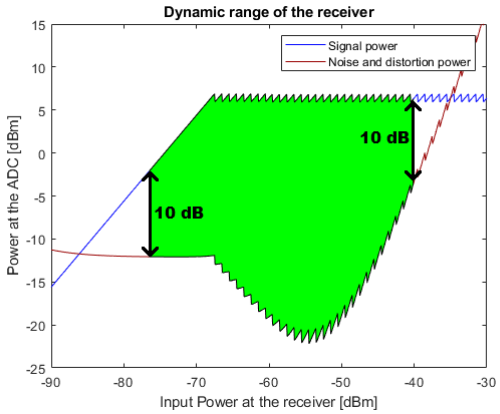

Figure 6.4: Dynamic input range of the receiver for the 4-column antenna case

Modulation	Min SNR_{peak} [dB]	Range [m]	Throughput [Gbit/s] code rates [11/15 14/15]
BPSK	9.6	0.2 - 22.4	[3.3 4.2]
QPSK	12.6	0.3 - 15.4	[6.6 8.4]
8-PSK	17.7	0.4 - 8.1	[9.9 12.6]
8-APSK	18.8	0.4 - 7.0	[9.9 12.6]
16-QAM	22.0	0.6 - 4.6	[13.2 16.8]

Table 6.8: Throughput and range for each modulation order for the 4-column antenna case and code rates [11/15 14/15]

As can be seen in figure 6.4, the range of possible input powers have shifted compared to the original case. This, in turn, alters the acceptable distances between the transmitter and receiver from 3.8-45.1 m to 2-21 m, approximately halving the maximum range. In table 6.8 a summary of the achievable throughput for the different ranges and modulation orders can be seen.

6.1.2 Combined Transmitter/Receiver architecture

In an architecture with a combined Tx/Rx, the same antenna is used for both reception and transmission. This requires the usage of switches to allow both the

Tx and Rx architecture access to the antenna itself, as they cannot both utilize it at the same time. These switches incur some additional attenuation, meaning the signal quality will be worsened. Using the same antenna on the Tx/Rx has the benefit of needing one less antenna array at each device, while enabling channel reciprocity. A schematic of the studied Tx/Rx architecture can be seen in figure 6.5

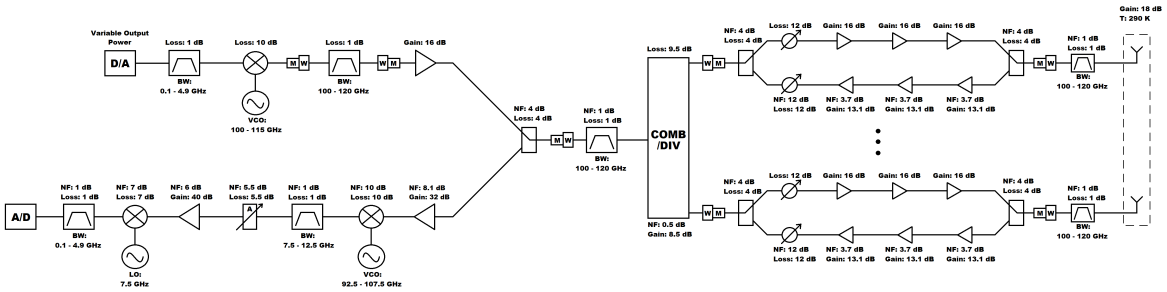

Figure 6.5: Block diagram of the examined combined transmitter/receiver communication system

Component	Power budget[dBm] f_c = [102.5,107.5,112.5,117.5] GHz	OIP3 [dBm] f_c = [102.5,107.5,112.5,117.5] GHz	Comment
D/A converter	[-16.1,-10.3,-13.5,-7.5]	-	
Filter 0.1-4.9 GHz	[-17.1,-11.3,-14.5,-8.5]	-	
Mixer 100-115 GHz	[-27.1,-21.3,-24.5,-18.5]	[16.0,14.0,12.0,10.0]	
Patch transition	[-27.3,-21.5,-24.7,-18.7]	[15.8,13.8,11.8,9.8]	Microstrip to waveguide
Filter 100-120 GHz	[-28.3,-22.5,-25.7,-19.7]	[14.8,12.8,10.8,8.8]	
E-plane transition	[-28.5,-22.7,-25.9,-19.9]	[14.6,12.6,10.6,8.6]	Waveguide to microstrip
Power amplifier	[-12.1,-7.0,-9.4,-4.9]	[26.6,25.8,24.5,22.1]	
Switch	[-16.1,-11.0,-13.4,-8.9]	[15.5,15.4,15.0,14.2]	
Patch transition	[-16.3,-11.2,-13.6,-9.1]	[15.3,15.2,14.8,14.0]	Microstrip to waveguide
Filter 100-120 GHz	[-17.3,-12.2,-14.6,-10.1]	[14.3,14.2,13.8,13.0]	
Power divider	[-26.8,-21.7,-24.1,-19.6]	[4.8,4.7,4.3,3.5]	
E-plane transition	[-27.0,-21.9,-24.3,-19.8]	[4.6,4.5,4.1,3.3]	Waveguide to microstrip
Switch	[-31.0,-25.9,-28.3,-23.8]	[0.5,0.4,0.0,-0.8]	
Phase shifter	[-43.0,-40.9,-43.3,-38.8]	[-11.5,-14.7,-15.0,-15.8]	
Power amplifier	[-26.6,-25.2,-26.8,-23.8]	[4.9,1.0,1.5,-0.8]	
Power amplifier	[-10.2,-9.5,-10.3,-8.8]	[20.5,16.5,17.6,14.0]	
Power amplifier	[6.2,6.2,6.2,6.2]	[27.9,27.6,27.0,25.2]	
Switch	[2.2,2.2,2.2,2.2]	[15.8,15.7,15.6,15.2]	
Patch transition	[2.0,2.0,2.0,2.0]	[15.6,15.5,15.4,15.0]	Microstrip to waveguide
Filter 100-120 GHz	[1.0,1.0,1.0,1.0]	[14.6,14.5,14.4,14.0]	
Antenna array	**[28.0,28.0,28.0,28.0]**	**[41.6,41.6,41.5,41.1]**	**EIRP**

Table 6.9: Transmitter power and OIP3 budget for frequencies [102.5, 107.5, 112.5 117.5] GHz, referred to output for the combined Transmitter/Receiver case

Component	Power budget [dBm] f_c = [102.5,107.5,112.5,117.5] GHz	Noise spectral density [dBm/Hz] f_c = [102.5,107.5,112.5,117.5] GHz	OIP3 [dBm] f_c = [102.5,107.5,112.5,117.5] GHz	Comment
Received signal power	[-72.9,-73.3,-73.7,-74.1]	-	-	
Antenna array	[-64.0,-64.4,-64.8,-65.1]	[-174.0,-174.0,-174.0,-174.0]	-	
Filter 100-120 GHz	[-65.0,-65.4,-65.8,-66.1]	[-174.0,-174.0,-174.0,-174.0]	-	
E-plane transition	[-65.2,-65.6,-66.0,-66.3]	[-174.0,-174.0,-174.0,-174.0]	-	Waveguide to microstrip
Switch	[-69.2,-69.6,-70.0,-70.3]	[-174.0,-174.0,-174.0,-174.0]	[16.5,16.5,16.5,16.5]	
LNA	[-56.1,-56.5,-56.9,-57.2]	[-157.2,-157.2,-157.2,-157.2]	[22.0,22.0,22.0,22.0]	
LNA	[-43.0,-43.4,-43.8,-44.1]	[-144.0,-144.0,-144.0,-144.0]	[22.6,22.6,22.6,22.6]	
LNA	[-29.9,-30.3,-30.7,-31.0]	[-130.9,-130.9,-130.9,-130.9]	[22.6,22.6,22.6,22.6]	
Phase shifter	[-41.9,-45.3,-45.7,-46.0]	[-142.8,-145.8,-145.8,-145.8]	[9.9,6.9,6.9,6.9]	
Switch	[-45.9,-49.3,-49.7,-50.0]	[-146.8,-149.8,-149.8,-149.8]	[5.5,2.7,2.7,2.7]	
Patch transition	[-46.1,-49.5,-49.9,-50.2]	[-147.0,-150.0,-150.0,-150.0]	[5.3,2.5,2.5,2.5]	Microstrip to waveguide
Combiner	[-37.5,-40.9,-41.3,-41.7]	[-147.5,-150.5,-150.5,-150.5]	[13.8,11.0,11.0,11.0]	
Filter 100-120 GHz	[-38.5,-41.9,-42.3,-42.7]	[-148.5,-151.5,-151.5,-151.5]	[12.8,10.0,10.0,10.0]	
E-plane transition	[-38.7,-42.1,-42.5,-42.9]	[-148.7,-151.7,-151.7,-151.7]	[12.6,9.8,9.8,9.8]	Waveguide to microstrip
Switch	[-42.7,-46.1,-46.5,-46.9]	[-152.7,-155.7,-155.7,-155.7]	[8.0,5.4,5.4,5.4]	
Gain stage	[-9.9,-14.7,-13.5,-16.9]	[-119.7,-123.9,-122.4,-125.3]	[28.2,28.7,27.5,26.7]	
Mixer 92.5-107.5 GHz	[-19.9,-24.7,-23.5,-26.9]	[-129.7,-133.9,-132.4,-135.3]	[13.9,12.7,10.9,9.2]	
Filter 7.5-12.5 GHz	[-20.9,-25.7,-24.5,-27.9]	[-130.7,-134.9,-133.4,-136.3]	[12.9,11.7,9.9,8.2]	
Attenuator	[-26.4,-31.2,-30.0,-33.4]	[-136.2,-140.4,-138.8,-141.8]	[7.4,6.2,4.4,2.7]	Equalize amplitude to achieve full range of A/D
Two power amplifiers	[13.6,8.8,10.0,6.6]	[-96.2,-100.4,-98.8,-101.8]	[38.4,38.2,37.9,37.4]	
Mixer 7.5-12.5 GHz	[6.6,1.8,3.0,-0.4]	[-103.2,-107.4,-105.8,-108.8]	[24.1,24.1,24.0,23.9]	
Filter 0.1-4.9 GHz	[5.6,0.8,2.0,-1.4]	[-104.2,-108.4,-106.8,-109.8]	[23.1,23.1,23.0,22.9]	
A/D converter	**[5.6,0.8,2.0,-1.4]**	**[-104.2,-108.4,-106.8,-109.8]**	**[23.1,23.1,23.0,22.9]**	

Table 6.10: Receiver power budget, Noise density and OIP3 at every stage of receiver for frequencies [102.5, 107.5, 112.5 117.5] GHz and a distance of 20 m, referred to output for the combined Transmitter/Receiver case

Parameter	Value f_c = [102.5 107.5 112.5 117.5] GHz
Transmitter third-order intermodulation product level	[-27.2,-27.1,-26.9,-26.1] dBc
Noise Level	[-7.4,-11.6,-10,-13.0] dBm
Receiver third-order intermodulation product level	[-35.1,-44.6,-42.1,-48.6] dBc
Signal-to-noise ratio	[13.0,12.4,12.0,11.6] dB

Table 6.11: Performance parameters for frequencies [102.5, 107.5, 112.5 117.5] GHz at a distance of 20 m, referred to output for the combined Transmitter/Receiver case

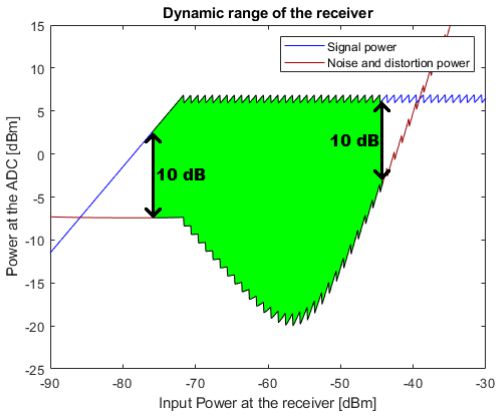

Figure 6.6: Dynamic input range of the receiver for the combined Tx/Rx case

Modulation	Min SNR_{peak} [dB]	Range [m]	Throughput [Gbit/s] code rates [11/15 14/15]
BPSK	9.6	0.6 - 30.5	[3.3 4.2]
QPSK	12.6	0.7 - 20.8	[6.6 8.4]
8-PSK	17.7	1.0 - 10.9	[9.9 12.6]
8-APSK	18.8	1.1 - 9.4	[9.9 12.6]
16-QAM	22.0	1.4 - 6.2	[13.2 16.8]

Table 6.12: Throughput and range for each modulation order for the combined antenna aperture case with code rates [11/15 14/15]

in order to be within the 10 dB SNR range for this architecture, a distance of between roughly 4.4 and 28.8 m is needed. In comparison to having separate antennas for transmission and reception of signals, this is an overall decrease in range, while the maximum attainable SNR for the link is approximately 15 dB compared to approximately 19 dB for the original case. This is due to the additional losses and thermal noise which the switches incur on the system, decreasing signal strength and increasing the noise level. it can also be seen that the transmitter OIP3 is significantly higher for this case compared to the separate architecture case in table 6.1. It should be noted, however, that this level still meets even the toughest EVM requirement set in table 4.2, meaning transmitter non-linearities will not be the main concern for this case. Lastly, a summary of the ranges and and throughput for them can be seen in table 6.12.

6.1.3 Comparison between the different variation of the communication system

The different variations of the communication exhibit different performance over different ranges. A comparison of the performance metrics is given in table 6.13 in order to easily highlight these performance differences.

Modulation	Min SNR_{peak} [dB]	Range [m] Initial case	Range [m] Smaller antenna case	Range [m] Switched antenna case	Throughput [Gbit/s] code rates [11/15 14/15]
BPSK	9.6	0.5 - 47.3	0.2 - 22.4	0.6 - 30.5	[3.3 4.2]
QPSK	12.6	0.6 - 32.6	0.3 - 15.4	0.7 - 20.8	[6.6 8.4]
8-PSK	17.7	0.8 - 17.2	0.4 - 8.1	1.0 - 10.9	[9.9 12.6]
8-APSK	18.8	0.9 - 14.7	0.4 - 7.0	1.1 - 9.4	[9.9 12.6]
16-QAM	22.0	1.2 - 9.8	0.6 - 4.6	1.4 - 6.2	[13.2 16.8]

Table 6.13: Corresponding operational range comparison between the different variations of the communication system with code rates [11/15 14/15].

6.1.4 FMCW radar system

The analysis of the considered FMCW radar is presented in this chapter. Changes in the Digital processing, Mixed signal and IF - RF blocks are made to the considered communication system in order to derive the architecture of the FMCW radar system. The considered FMCW radar system architecture is presented in figure 6.7.

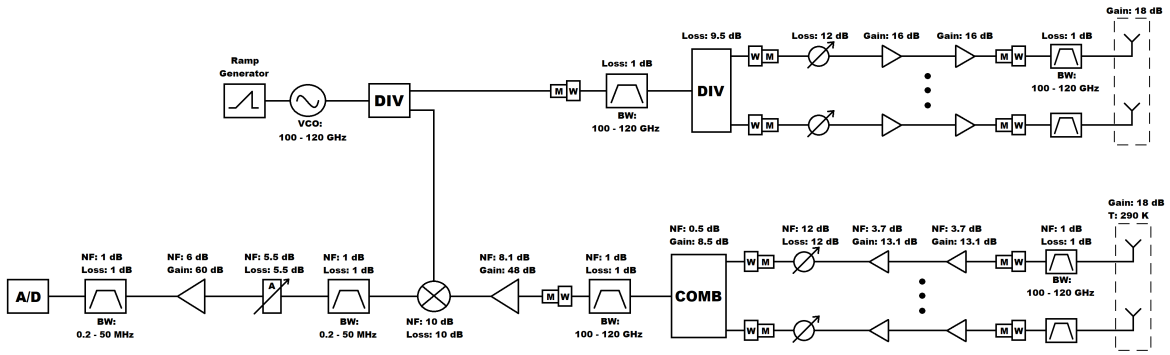

Figure 6.7: Block diagram of the examined FMCW radar system

As the FMCW radar is designed to appeal to automotive applications certain signal design parameters are chosen to fit the intended applications. These design parameters are presented in table 6.14.

Parameter	Value
Sweep bandwidth	500 MHz
Chirp period	13.2 μs
Number of chirps	110
Sampling frequency	100 MHz
Target radar cross-section	10 m^2

Table 6.14: Design parameters for the considered FMCW radar system.

Component	Power budget[dBm] f_c = [102.5,107.5,112.5,117.5] GHz	OIP3 [dBm] f_c = [102.5,107.5,112.5,117.5] GHz	Comment
VCO	[-18.7,-14.3,-15.9,-12.9]	-	
Power divider	[-21.7,-17.3,-18.9,-15.9]	-	
Patch transition	[-21.9,-17.5,-19.1,-16.1]	-	Microstrip to waveguide
Filter 100-120 GHz	[-22.9,-18.5,-20.1,-17.1]	-	
Power divider	[-32.4,-28.0,-29.6,-26.6]	-	
E-plane transition	[-32.6,-28.2,-29.8,-26.8]	-	Waveguide to microstrip
Phase shifter	[-44.6,-43.2,-44.8,-41.8]	[18.0,15.0,15.0,15.0]	
Power amplifier	[-28.2,-27.5,-28.3,-26.8]	[27.5,27.0,26.4,25.6]	
Power amplifier	[-11.8,-11.8,-11.8,-11.8]	[28.4,29.3,27.9,27.3]	
Patch transition	[-12.0,-12.0,-12.0,-12.0]	[28.2,29.1,27.7,27.1]	Microstrip to waveguide
Filter 100-120 GHz	[-13.0,-13.0,-13.0,-13.0]	[27.2,28.1,26.7,26.1]	
Antenna array	**[14.0,14.0,14.0,14.0]**	**[54.2,55.1,53.7,53.1]**	**EIRP**

Table 6.15: Transmitter power and OIP3 budget for frequencies [102.5, 107.5, 112.5 117.5] GHz, referred to output for the FMCW radar case.

Component	Power budget [dBm] f_c = [102.5,107.5,112.5,117.5] GHz	Noise spectral density [dBm/Hz] f_c = [102.5,107.5,112.5,117.5] GHz	OIP3 [dBm] f_c = [102.5,107.5,112.5,117.5] GHz	Comment
Received signal power	[-139.7,-140.1,-140.5,-140.9]	-	-	
Antenna array	[-130.7,-131.1,-131.5,-131.9]	[-174.0,-174.0,-174.0,-174.0]	-	
Filter 100-120 GHz	[-131.7,-132.1,-132.5,-132.9]	[-174.0,-174.0,-174.0,-174.0]	-	
E-plane transition	[-131.9,-132.3,-132.7,-133.1]	[-174.0,-174.0,-174.0,-174.0]	-	Waveguide to microstrip
LNA	[-118.8,-119.2,-119.6,-120.0]	[-157.2,-157.2,-157.2,-157.2]	[22.8,22.8,22.8,22.8]	
LNA	[-105.7,-106.1,-106.5,-106.9]	[-144.0,-144.0,-144.0,-144.0]	[22.6,22.6,22.6,22.6]	
Phase shifter	[-117.7,-121.1,-121.5,-121.9]	[-155.9,-158.8,-158.8,-158.8]	[9.9,6.9,6.9,6.9]	
Patch transition	[-117.9,-121.3,-121.7,-122.1]	[-156.1,-159.0,-159.0,-159.0]	[9.7,6.7,6.7,6.7]	Microstrip to waveguide
Combiner	[-109.4,-112.8,-113.2,-113.6]	[-156.6,-159.5,-159.5,-159.5]	[18.2,15.2,15.2,15.2]	
Filter 100-120 GHz	[-110.4,-113.8,-114.2,-114.6]	[-157.6,-160.5,-160.5,-160.5]	[17.2,14.2,14.2,14.2]	
E-plane transition	[-110.6,-114.0,-114.4,-114.8]	[-157.8,-160.7,-160.7,-160.7]	[17.0,14.0,14.0,14.0]	Waveguide to microstrip
Gain stage	[-61.4,-66.9,-64.9,-69.8]	[-108.0,-112.6,-110.2,-114.7]	[28.4,29.4,27.9,27.4]	
Mixer 92.5-107.5 GHz	[-71.4,-76.9,-74.9,-79.8]	[-118.0,-122.6,-120.2,-124.7]	[14.0,12.9,11.0,9.3]	
Filter 7.5-12.5 GHz	[-72.4,-77.9,-75.9,-80.8]	[-119.0,-123.6,-121.2,-125.7]	[13.0,11.9,10.0,8.3]	
Attenuator	[-77.9,-83.4,-81.4,-86.3]	[-124.5,-129.1,-126.7,-131.2]	[7.5,6.4,4.5,2.8]	Equalize amplitude to achieve full range of A/D
Two power amplifiers	[-17.9,-23.4,-21.4,-26.3]	[-64.5,-69.1,-66.7,-71.2]	[39.0,38.9,38.9,38.9]	
Filter 0.1-4.9 GHz	[-18.9,-24.4,-22.4,-27.3]	[-65.5,-70.1,-67.7,-72.2]	[38.0,37.9,37.9,37.9]	
A/D converter	**[-18.9,-24.4,-22.4,-27.3]**	**[-65.5,-70.1,-67.7,-72.2]**	**[38.0,37.9,37.9,37.9]**	

Table 6.16: Receiver power budget, Noise density and OIP3 at every stage of receiver for frequencies [102.5, 107.5, 112.5 117.5] GHz and a distance of 20 m, referred to output for the FMCW radar case

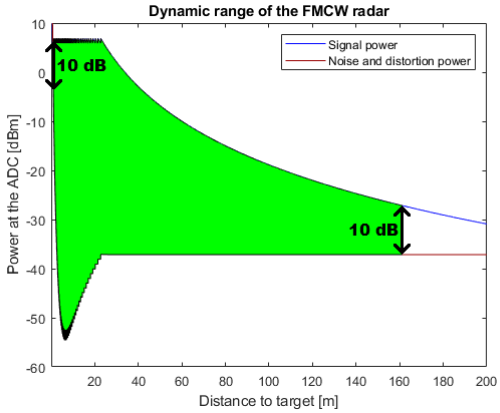

Figure 6.8: Signal power versus noise and distortion power as a function of target distance for the FMCW radar system operating at a center frequency of 102.5 GHz.

Figure 6.8 illustrates the ranges where an sufficient signal-to-noise ratio is achievable. The target ranges that do not achieve a sufficient signal-to-noise ratio limits the minimum and maximum target ranges. The minimum target range is limited by the distortion power while the maximum range is limited by the thermal noise. The performance parameters of the considered FMCW radar system is presented in table 6.17.

Parameter	Value
Minimum detection range	1.0 m
Maximum detection range	161.1 m
Range resolution	± 0.3 m
Maximum unambiguous velocity	55.4 m/s
Velocity resolution	± 1.0 m/s

Table 6.17: Performance parameters for the FMCW radar system operating at a center frequency of 102.5 GHz.

7
Discussion

A realistic link budget considering both thermal noise and non-linearities for three variations of a communication system, as well as for an FMCW radar has been made. This has been done on component-level, allowing the budgets to be used in order to identify the components which deteriorate quality the most. In addition to this, a table with modulations and at what range they are operable has been provided for each of the communication system variations. This provides easily digestible tables for the average reader, while still providing important details to the more advanced reader. A section dedicated to the difference in requirements between a communication system and FMCW radar has also been written. Additionally, two tables detailing design- and performance-parameters is given for the FMCW radar. The implications of this work is that communication on sub-THz frequencies is likely viable using the developed hardware. The link-budget of the system and all its variations seem promising, achieving high-rate wireless communication at reasonable distances, although it is often not spectrally efficient due to the higher modulation orders not always being available. The communication link is worse off for the different variations, which is reasonable given they have worse hardware conditions compared to the original case. The work also assumes that the channel is quite good, since shadowing is brutal on frequencies this high. Because of this, the link quality will likely, although not investigated, struggle with transitions between indoor and outdoor unless there is a relay between the environments.

7.1 Realistic component values

When using components in calculations, their data sheets have been consulted for parameter values. When possible, parameter graphs with values dependent on frequency were consulted to obtain accurate values for the different frequencies. Otherwise, the stated typical values for the correct frequency intervals in the data sheets has been used. This approach leaves some room for error as the typical values may deviate some decibels from the actual values at specific points within the frequency range. By using a variable attenuator, small deviations in component gain become less significant to the signal-to-noise ratio. This is because the variable attenuator can either attenuate the signal further or less depending on the signal strength at the input, effectively compensating for the deviation in gain. When it comes to the component noise figures, the earlier components in the receiver will have the most significant impact on the over-all system noise level. Therefore, deviations in noise figures for components later in the receiver will not effect the over-all system noise

level in a noticeable degree. The opposite can be said about the OIP3 effect on the system. Contrary to the noise figure, its effects are instead the most prevalent toward the end of the chain, as that is where the signal level is at its largest. Due to this, the deviations in OIP3 levels for components earlier in the chain will not have a significant impact on the system distortion level.

7.2 Recommendations for future work

This work has not conducted any investigation about calibration for the system. No work regarding manufacturing tolerances has been carried out either. These types of studies would add significant value to the work, meaning it would be wise to carry out such analyses for future work. This paper has not had a large focus on the interfaces between components either, although some interfacing has been considered in the form of micro strip to waveguide transitions. However, micro strip losses between the components have not been considered. In future work, a more rigorous consideration of these effects could for example be made using simulations in `ANSYS` or `COMSOL`.

If the work is to be extended or carried out by somebody else, much could be developed upon or added aside from what is already mentioned. In order to obtain a more realistic link-model, improved modeling of the channel is of importance. In this paper, the channel model assumes a constant noise level, along with constant shadow fading. To get a more accurate model, scattering and multi-path for the specific environment should be taken into account. Different environments could also be compared in order to assess their viability. To further describe the impact of channels on the link quality, it could be of use to simulate transmission over a relevant channel with and without the different types of coding. Their performance could then be compared to obtain the coding gain given the conditions which it was simulated for. Doing this would allow more accurate decisions on coding to be made for different environments, enhancing performance.

In calculating the achievable rates of the system, overhead from signaling and pilot-words have not been considered. These factors are dependent on the used transmission protocols, meaning they have to be pointed out in order to achieve a throughput calculation which take such effects into consideration. Neither did the throughput calculations consider processing time at the transmitter and receiver. Another important aspect which could be considered is the effect which a lower bandwidth would have on the total noise in the system, and if it could even allow higher rates due to the decrease in total noise over the bandwidth. If so, transmitting more information with less resources would be possible. Additionally, it seems easier to develop hardware with a more restricted bandwidth compared to the case at hand, meaning there might also be an opportunity for some simplification in their design or improvement in performance.

This work assumes that the only bound in terms of power is that no more than 10 mW is to be transmitted over the channel. In reality, the components may be restricted in the amount of power passing through them due to heat dissipation. It is also possible that the device may be restricted by a limited-capacity battery, meaning the operating time could constrain the available power of the device, although it is

not considered in this work.
The FMCW radar system considered in this project achieves a sufficient signal-to-noise ratio at the intended target ranges. However, the analysis conducted in this project could still be improved upon. The result show that the current signal level is highly dependent on the range to the target. By implementing filters with frequency dependent slopes, the signal can have a range independent level. With this, it would be possible to draw conclusions about the radar cross-section of the observed targets from the signal level. Additionally, building a prototype for the FMCW radar would be helpful to verify its functioning and identify practical problems with its realization. It could also help identify problematic design choices, allowing changes to be made.

8
Conclusion

The conclusion from this work is that a communication and radar system indeed seems possible beyond 100 GHz, although some parameters such as power consumption and efficiency have not been fully investigated. Because of this, work could still be done to further analyze the potential system. Such further analysis would allow more accurate estimations of when specific modulations are possible, yielding more accurate approximations of obtainable rates. The existence of other hardware and channel impairments mean there is still ample room for signals to achieve an SNR lower than what is aimed for. However, some possibilities still exist to increase the SNR, such as using coding and considering a different architecture or different components. Lastly, the investigated communication systems achieves high data rates, even with spectrally inefficient modulations such as BPSK. For some range intervals, it functions with higher modulation orders, meaning high throughput is possible.

Another conclusion is that a FMCW radar could be constructed using a similar architecture as the considered communication system. A large part of the communication system architecture can be kept the same while adapting the system for automotive radar applications. With the necessary configurations of the signal parameters, the system achieves an acceptable signal-to-noise ratio for the intended range.

All of the investigated communication systems function in theory, although they achieve different ranges. The baseline case, where two separate 8-column antennas are used, achieves the best overall performance. When compared to a 4-column case, the maximum range is approximately 55% longer, making it more suited to long range communication. This does however come at the cost of a more complex and larger, likely more expensive antenna. Another trade-off which can be made is to utilize a shared antenna for both transmission and reception. For this case, the trade-off is made by having switches in the system, which introduces some additional noise early on in the system chain, deteriorating signal-to-noise ratio. Utilizing a shared antenna also means that there is less flexibility for the system, as it must then utilize a TDD scheme and the communicating devices require more synchronization between one another. However, by utilizing a shared antenna it is possible to exploit channel reciprocity.

Bibliography

[1] S.-E. Österberg *et al.*, *Frekvenser i samhällets tjänst*, 2018.

[2] N. Telecommunications and N. Information Administration, *United states frequency allocation chart*, 2016. [Online]. Available: `https://www.ntia.doc.gov/page/2011/united-states-frequency-allocation-chart` (visited on 05/20/2022).

[3] V. Petrov, T. Kurner, and I. Hosako, "Ieee 802.15.3d: First standardization efforts for sub-terahertz band communications toward 6g", *IEEE Communications Magazine*, vol. 58, no. 11, pp. 28–33, 2020. DOI: `10.1109/MCOM.001.2000273`.

[4] T. S. Rappaport *et al.*, "Wireless Communications and Applications Above 100 GHz: Opportunities and Challenges for 6G and Beyond", *IEEE Access*, vol. 7, pp. 78 729–78 757, 2019. DOI: `10.1109/ACCESS.2019.2921522`.

[5] X. Li, J. Xiao, and J. Yu, "Long-distance wireless mm-wave signal delivery at w-band", *Journal of Lightwave Technology*, vol. 34, no. 2, pp. 661–668, 2016. DOI: `10.1109/JLT.2015.2500581`.

[6] X. Li, J. Xiao, and J. Yu, "Long-distance wireless mm-wave signal delivery at w-band", *Journal of Lightwave Technology*, vol. 34, no. 2, pp. 661–668, 2016. DOI: `10.1109/JLT.2015.2500581`.

[7] H. Sarieddeen, M.-S. Alouini, and T. Y. Al-Naffouri, "An overview of signal processing techniques for terahertz communications", *Proceedings of the IEEE*, vol. 109, no. 10, pp. 1628–1665, 2021. DOI: `10.1109/JPROC.2021.3100811`.

[8] CelcticNext. "Project entry100ghz". (2021), [Online]. Available: `https://www.celticnext.eu/project-entry100ghz/` (visited on 05/20/2022).

[9] M. B. Gérard Maral, *Satellite Communication Systems, Systems, Techniques and technology*. John Wiley & Sons, 2009, ISBN: 978-0-470-71458-4.

[10] C. Kestel, M. Herrmann, and N. When, "When channel coding hits the implementation wall", in *2018 IEEE 10th International Symposium on Turbo Codes Iterative Information Processing (ISTC)*, 2018, pp. 1–6. DOI: `10.1109/ISTC.2018.8625324`.

[11] J. B. Anderson, *Digital Transmission Engineering*. A John Wiley & Sons, INC, 2005, ISBN: 978-0-471-69464-9.

[12] R. A. Gibby and J. W. Smith, "Some extensions of nyquist's telegraph transmission theory", *The Bell System Technical Journal*, vol. 44, no. 7, pp. 1487–1510, 1965. DOI: 10.1002/j.1538-7305.1965.tb04188.x.

[13] M. Shehata *et al.*, "IEEE 802.15.3d-Compliant Waveforms for Terahertz Wireless Communications", *Journal of Lightwave Technology*, vol. 39, no. 24, pp. 7748–7760, 2021. DOI: 10.1109/JLT.2021.3113310.

[14] H. Solis-Estrella and A. G. Orozco-Lugo, "Carrier Frequency Offset Estimation in OFDMA using Digital Filtering", *IEEE Wireless Communications Letters*, vol. 2, no. 2, pp. 199–202, 2013. DOI: 10.1109/WCL.2013.011713.120872.

[15] F. Ling and J. Proakis, *Synchronization in Digital Communication Systems*. Cambridge University Press, 2017. DOI: 10.1017/9781316335444.

[16] C. Wang *et al.*, "Joint estimation of carrier frequency and phase offset based on pilot symbols in quasi-constant envelope ofdm satellite systems", *China Communications*, vol. 14, no. 7, pp. 1–11, 2017. DOI: 10.1109/CC.2017.8019135.

[17] A. Goldsmith, *Wireless Communications*. Cambridge University Press, 2005, ISBN: 9780521837163.

[18] F. Maloberti, *Data Converters*. Springer, 2007, ISBN: 978-0-387-32486-9.

[19] S. Pavan, R. Schreier, and G. C. Temes, "Sampling, oversampling, and noise-shaping", in *Understanding Delta-Sigma Data Converters*. 2017, pp. 27–61. DOI: 10.1002/9781119258308.ch2.

[20] *12-bit, 10.25 gsps, jesd204b, rf analog-to-digital converter*, AD9213, Rev.A, Analog Devices, 2020.

[21] D. M. Pozar, *Microwave engineering; 1st ed.* John Wiley & sons, 2000.

[22] T. J. Rouphael, "Chapter 4 - system nonlinearity", in *Wireless Receiver Architectures and Design*, T. J. Rouphael, Ed., Boston: Academic Press, 2014, pp. 179–261, ISBN: 978-0-12-378640-1. DOI: https://doi.org/10.1016/B978-0-12-378640-1.00004-4. [Online]. Available: https://www.sciencedirect.com/science/article/pii/B9780123786401000044.

[23] R. S. Elliott, *Antenna Theory and Design, Revised Edition*. John Wiley & Sons, 2003, ISBN: 9780470544174.

[24] P.-S. Kildal, *Foundations of Antenna Engineering: A Unified Approach for Line-of-Sight and Multipath*. 2015.

[25] K. Haneda *et al.*, "5g 3gpp-like channel models for outdoor urban microcellular and macrocellular environments", in *2016 IEEE 83rd Vehicular Technology Conference (VTC Spring)*, 2016, pp. 1–7. DOI: 10.1109/VTCSpring.2016.7503971.

[26] Y. Xing and T. S. Rappaport, "Propagation measurement system and approach at 140 ghz-moving to 6g and above 100 ghz", in *2018 IEEE Global Communications Conference (GLOBECOM)*, 2018, pp. 1–6. DOI: 10.1109/GLOCOM.2018.8647921.

[27] S. L. H. Nguyen *et al.*, "Comparing radio propagation channels between 28 and 140 ghz bands in a shopping mall", in *2018 12th European Conference on Antennas and Propagation (EuCAP)*, 2017. DOI: https://doi.org/10.48550/arXiv.1712.09438.

[28] "IEEE Standard for High Data Rate Wireless Multi-Media Networks–Amendment 2: 100 Gb/s Wireless Switched Point-to-Point Physical Layer", *IEEE Std 802.15.3d-2017 (Amendment to IEEE Std 802.15.3-2016 as amended by IEEE Std 802.15.3e-2017)*, pp. 1–55, 2017. DOI: 10.1109/IEEESTD.2017.8066476.

[29] Mathworks, *Bit error rate analysis*, Accessed: 2022-04-29, 2022. [Online]. Available: https://se.mathworks.com/help/comm/ref/biterrorrateanalysis-app.html.

[30] Mathworks, *Template for simulation function*, Accessed: 2022-04-29, 2022. [Online]. Available: https://se.mathworks.com/help/comm/ug/use-bit-error-rate-analysis-app.html#a1061397196b2.

[31] A. M. A. Ali *et al.*, "A 12-b 18-gs/s rf sampling adc with an integrated wideband track-and-hold amplifier and background calibration", *IEEE Journal of Solid-State Circuits*, vol. 55, no. 12, pp. 3210–3224, 2020. DOI: 10.1109/JSSC.2020.3023882.

[32] M. Zhang *et al.*, "16.2 a 4× interleaved 10gs/s 8b time-domain adc with 16× interpolation-based inter-stage gain achieving gt;37.5db sndr at 18ghz input", in *2020 IEEE International Solid- State Circuits Conference - (ISSCC)*, 2020, pp. 252–254. DOI: 10.1109/ISSCC19947.2020.9062986.

[33] *WILD FMC+ DME1 ADC & DAC – WWDME1*, Annapolis Micro Systems. [Online]. Available: https://www.annapmicro.com/products/wild-fmc-dme1/, accessed 15/03/2022.

[34] W. Kester, *Adc noise figure—an often misunderstood and misinterpreted specification*, Rev.B, Analog Devices, 2014.

[35] B. Lizon, *Fundamentals of precision adc noise analysis*, Texas Instruments, Sep. 2020.

[36] X. Bo, D. Wenbin, and H. Minmin, "A subharmonic mixer at W band", in *2012 International Conference on Microwave and Millimeter Wave Technology (ICMMT)*, vol. 3, 2012, pp. 1–3. DOI: 10.1109/ICMMT.2012.6230211.

[37] F. Meng, Y. Chen, and Y. Fang, "A W-band Fundamental Mixer MMIC Using Planar Schottky Diode", in *2020 Cross Strait Radio Science Wireless Technology Conference (CSRSWTC)*, 2020, pp. 1–3. DOI: 10.1109/CSRSWTC50769.2020.9372726.

[38] Y. Liu *et al.*, "A schottky diodes based w-band 4th-harmonic mixer", in *2017 International Applied Computational Electromagnetics Society Symposium (ACES)*, 2017, pp. 1–2.

[39] J. T. Do, Y. Bey, and X. Liu, "A high-q w band tunable bandpass filter", in *2016 IEEE MTT-S International Microwave Symposium (IMS)*, 2016, pp. 1–4. DOI: 10.1109/MWSYM.2016.7540094.

[40] X. Shang *et al.*, "W-band waveguide filters fabricated by laser micromachining and 3-d printing", *IEEE Transactions on Microwave Theory and Techniques*, vol. 64, no. 8, pp. 2572–2580, 2016. DOI: 10.1109/TMTT.2016.2574839.

[41] K. Zhou *et al.*, "W-band dual-band quasi-elliptical waveguide filter with flexibly allocated frequency and bandwidth ratios", *IEEE Microwave and Wireless Components Letters*, vol. 28, no. 3, pp. 206–208, 2018. DOI: 10.1109/LMWC.2018.2796840.

[42] Y. Xing *et al.*, "Indoor wireless channel properties at millimeter wave and subterahertz frequencies", Dec. 2019, pp. 1–6. DOI: 10.1109/GLOBECOM38437.2019.9013236.

[43] A. Dias, D. Bateman, and K. Gosse, "Impact of rf front-end impairments and mobility on channel reciprocity for closed-loop multiple antenna techniques", in *2004 IEEE 15th International Symposium on Personal, Indoor and Mobile Radio Communications (IEEE Cat. No.04TH8754)*, vol. 2, 2004, 1434–1438 Vol.2. DOI: 10.1109/PIMRC.2004.1373935.

[44] S.-F. Chao *et al.*, "A 50 to 94-ghz cmos spdt switch using traveling-wave concept", *IEEE Microwave and Wireless Components Letters*, vol. 17, no. 2, pp. 130–132, 2007. DOI: 10.1109/LMWC.2006.890339.

[45] R.-B. Lai, J.-J. Kuo, and H. Wang, "A 60–110 ghz transmission-line integrated spdt switch in 90 nm cmos technology", *IEEE Microwave and Wireless Components Letters*, vol. 20, no. 2, pp. 85–87, 2010. DOI: 10.1109/LMWC.2009.2038519.

[46] F. Kaltenberger *et al.*, "Relative channel reciprocity calibration in mimo/tdd systems", Jul. 2010, pp. 1–10.

[47] M. Richards *et al.*, *Principles of Modern Radar: Basic Principles, Volume 1* (Electromagnetics and Radar). Institution of Engineering and Technology, 2010, ISBN: 9781891121524. [Online]. Available: https://books.google.se/books?id=nD7tGAAACAAJ.

[48] E. Bel Kamel, A. Peden, and P. Pajusco, "RCS modeling and measurements for automotive radar applications in the W band", in *EUCAP 2017 : 11th European conference on antennas and propagation*, Paris, France, Mar. 2017, pp. 2445–2449. DOI: 10.23919/EuCAP.2017.7928266. [Online]. Available: https://hal.archives-ouvertes.fr/hal-01574836.

DEPARTMENT OF SOME SUBJECT OR TECHNOLOGY
CHALMERS UNIVERSITY OF TECHNOLOGY
Gothenburg, Sweden
www.chalmers.se

CHALMERS
UNIVERSITY OF TECHNOLOGY